Ultraviolet Dosage and Decontamination Efficacy was Widely Variable across 14 UV Devices after Testing a Dried Enveloped Ribonucleic Acid Virus Surrogate for SARS-CoV-2

Running title: UV Decontamination, Enveloped Virus

Tony L. Buhr[1], Erica Borgers-Klonkowski[1], Bradford W. Gutting[1], Emlyn E. Hammer[1], Shelia M. Hamilton[1], Brett M. Huhman[2], Stuart L. Jackson[2], Neil L. Kennihan[1], Samuel D. Lilly[1], John D. Little, Jr[2], Brooke B. Luck[1], Emily A. Matuczinski[1], Charles T. Miller[1], Rachel E. Sides[1], Vanessa L. Yates[1], Alice A. Young[1]

[1]Naval Surface Warfare Center-Dahlgren Division, Concepts and Experimentation Branch (B64), Dahlgren, VA USA

[2]Naval Research Laboratory (Plasma Physics Division), Washington, DC USA

Correspondence:
Tony L. Buhr, PhD
tony.l.buhr.civ@us.navy.mil

Keywords: Φ6, enveloped virus, decontamination, ultraviolet (UV), SARS-CoV-2, COVID-19

Abstract

Aims: The dosages and efficacy of 14 ultraviolet (UV) decontamination technologies were measured against a SARS-CoV-2 surrogate virus that was dried on to different materials for lab and field testing.

Methods and Results: A live enveloped, ribonucleic acid (RNA) virus surrogate for SARS-CoV-2 was dried on stainless steel 304 (SS304), Navy Top Coat-painted SS304 (NTC), cardboard, polyurethane, polymethyl methacrylate (PMMA), and acrylonitrile butadiene styrene (ABS) at > 8.0 $\log_{10}$ plaque-forming units (PFU) per test coupon. The coupons were then exposed to UV radiation during both lab and field testing. Commercial and prototype UV-emitting devices were measured for efficacy: 4 handheld devices, 3 room/surface-disinfecting machines, 5 air-disinfection devices, and 2 larger custom-made machines. UV device dosages ranged from 0.01-729 mJ cm^{-2}. Anti-viral efficacy among the different UV devices ranged from no decontamination up to nearly achieving sterilization. Importantly, cardboard required far more dosage than SS304.

Conclusions: Enormous variability in dosage and efficacy was measured among the different UV devices. Porous materials limit the utility of UV decontamination.

Significance and Impact of the Study: UV devices have wide variability in dosages, efficacy, hazards, and UV output over time indicating that each UV device needs independent technical measurement and assessment for product development, prior to, and during use.

INTRODUCTION

Tremendous attention was directed at the subject of UV decontamination during the COVID-19 pandemic, although UV devices are best used to augment other sanitation techniques rather than for stand-alone decontamination as successful use of UV depends on various environmental and technical factors (Raiszadeh and Adeli 2020; Memarzadeh 2021). Numerous devices that incorporate UV sources including handheld, room decontamination devices, and water treatment devices are available on the market to decontaminate air, water, and surface materials. Variability in UV devices is extensive and includes differences in electronics, bulbs, power, and product designs. The distance from UV sources at which decontamination/inactivation occurs is also widely variable ranging from a couple of centimeters to a couple of meters. UV sources also differ and include mercury (Hg), krypton chloride (KrCl), xenon (Xe), and various light emitting diodes (LED), which range in wavelength, and there are several different manufacturers. Additionally, although Hg bulbs are the most common, Hg bulb dosage significantly varies over time after the Hg bulb is turned on. Hg also comes with the risk of toxicity, although that risk is similar to fluorescent light bulbs. The variability in these decontamination devices is further complicated by variability in test methods, which include different virus preparation methods, tests with unpurified vs. purified virus, tests with wet virus or dried virus, presence of organic debris, and differences in porosity of surface materials. Assessments of UV for decontamination must also take into account maintenance since UV sources need to be cleaned in order to maintain dosage (United States Food and Drug Administration 2021; United States Environmental Protection Agency 2021).

UV radiation, particularly UV-C, is a known microbe disinfectant for air, water, and nonporous surfaces (United States Food and Drug Administration 2021; United States Environmental Protection Agency 2021). UV-C primarily inactivates microbes including viruses if they are directly exposed to the UV radiation. Therefore inactivation is far less effective if a microbe is associated with soil, dust, oils, any type of host cell debris, or if it is embedded in porous materials (United States Food and Drug Administration 2021). This is particularly relevant for obligate pathogens like viruses which are naturally associated with host cell components and body fluids: mucus in the case of respiratory virus like SARS-CoV-2 (Aps and Marten 2005; Heimbuch et al. 2013; Vejerano and Marr 2018). The effectiveness of UV-C lamps in inactivating environmentally relevant SARS-CoV-2 virus is unknown because there is limited consistent and/or reliable published data about the wavelength, dose, and duration of UV-C radiation required to inactivate the SARS-CoV-2 virus, particularly in its natural (unpurified) state (United States Food and Drug Administration 2021; United States Environmental Protection Agency 2021). This is true of all viruses because UV efficacy is further complicated by the fact that methods for virus preparation and testing, particularly enveloped viruses, are

highly variable among laboratories (Hadi et al. 2020). Purified enveloped viruses are often tested in laboratories, even though these viruses only exist naturally when associated with host cell components and debris in nature, and they can be compromised during purification (Cox and Wathes 1995).

The stability of viral particles in the environment depends on temperature and humidity, as well as characteristics of the virus itself as it is shed from the host (Cox and Wathes 1995). Human respiratory droplets are mainly composed of mucus (salt, mucin glycoprotein, and lipids (surfactants)), and these components can shield the virus from UV and affect decontamination kinetics (Vejerano and Marr 2018; Hadi et al. 2020). The mean size of infectious, respirable particles is 4 um for a 50% probability of a thoracic deep lung deposition (Brown et al. 2013). Particles >10 um don't go past the larynx and particles <1 um have lower probabilities of deposition (Brown et al. 2013; Hofer et al. 2021). Measurements of SARS-CoV-2 respiratory droplets are typically 0-1 virions per speech particle, and the water in SARS-CoV-2 respiratory particles evaporates within seconds to generate dry particles around 4 um, right at the respirable size range (Stadnytskyi et al. 2020). Hence, the virus respiratory size is much larger than the size of a naked coronavirus, which are 78 nm for SARS-CoV (Goldsmith et al. 2004) and can range from 50-200 nm (Masters 2006). A volume/volume calculation with a 78 nm virus and 4 um particle equates to >99.999% mucus and <0.001% virus per particle and sets a minimum target on the ratio of debris to virus expected for decontamination testing. This only accounts for debris in respiratory particles and does not account for additional debris that might be found on surfaces. In addition, enveloped viruses are more stable in dry conditions compared to wet environments (Cox and Wathes 1995; Chan et al. 2011; Buhr et al. 2020; Hadi et al. 2020; van Doremalen et al., 2013), and drying viruses via lyophilization is frequently used to stabilize virus for long-term storage (Greiff et al. 1954; Greiff and Richtel 1966; Malenovska 2014). Hence decontamination kinetics can also be greatly influenced depending on whether the test microbes are wet or dry. Rhinotillexis (nose-picking) creates additional environmental loads of infectious virus, which is also composed of mucus mixed with unpurified virus and varying levels of free water (Hendley et al. 1973; Weber et al. 2008).

In addition to methods gaps to define, characterize, and standardize SARS-CoV-2 virus debris composition and drying, standardized methods for reproducibly preparing high titers (>10 $\log_{10}$ of virus ml^{-1} of culture medium at the time of virus harvest) of SARS-CoV-2 for testing without artificial post-harvest cleaning and concentration steps are needed for statistical confidence and to match virus levels in the environment. Furthermore, there were/are urgent needs during the COVID-19 pandemic to test decontamination devices, like UV, in field tests outside of laboratory containment. Viruses that fall under higher World Health Organization (WHO) biosafety level (BSL) classifications such as SARS-CoV-2 (BSL-3) and its BSL-2 surrogate coronaviruses (ASTM International 2020) cannot be widely used in field tests because of cost, time, and safety constraints. For field testing, the enveloped virus surrogate Φ6 was previously used to make "live/dead" Φ6 test indicators to directly test and compare decontamination efficacy across lab and field tests (Buhr et al. 2020).

Surrogates are often used as models in studies of decontamination for highly infectious pathogens. Bacteriophages are useful for this purpose as they are similar in terms of morphology, behavior in the environment, and surface properties, but are BSL-1 and easier to isolate at high titers (>10 $\log_{10}$ ml^{-1} without virus purification and concentration) for testing than mammalian

120 viruses (Gallandat and Lantagne 2017). Among bacteriophages, Φ6 has been identified as a
121 preferred surrogate for enveloped viruses including influenza and SARS-CoV-2 (Bibby et al.
122 2015; Gallandat and Lantagne 2017; Vejerano and Marr 2018; Buhr et al. 2020; Fedorenko et al.
123 2020). *Pseudomonas* virus Φ6 is a BSL-1 enveloped RNA virus originally isolated in a bean
124 field as a lytic virus that infects the plant pathogenic bacterium *Pseudomonas syringae* pathovar
125 *phaseolicola* (Vidaver et al. 1973; Van Etten et al. 1976; Mindich 2004). The Φ6 envelope
126 structure is similar to many other enveloped viruses as the envelope consists of a
127 glycoprotein/protein-embedded lipid membrane, and the host cell has similar temperature
128 sensitivity to mammalian cells at around 40°C. This is important since the envelope components
129 are considered a target for inactivation by many different decontaminants including UV
130 radiation, particularly at 222 nm (McDonnell and Burke 2011; Wiggington et al. 2012; Hadi et
131 al. 2020; United States Food and Drug Administration 2021). Φ6 is a 13.5 kb double-stranded
132 RNA (dsRNA) phage (Mindich 2004), and spherical (80-100 nm diameter) with structural
133 similarity to coronaviruses (50-200 nm diameter). The 13.5 kb dsRNA genome, the equivalent of
134 27 kb of single-stranded RNA (ssRNA), is comparable to the 26-32 kb of ssRNA in
135 coronaviruses. In theory, a surrogate virus should have a similar number of adjacent pyrimidines
136 compared to SARS-CoV-2 since pyrimidine dimerization is considered an important mechanism
137 of UV inactivation (e.g. Heßling et al. 2020). Based on pyrimidine target numbers only, Φ6
138 (6,613 adjacent pyrimidine pairs) and SARS-CoV-2 (7,600 pairs) should have similar UV
139 sensitivity, although ssRNA may be slightly more sensitive than dsRNA due to the potential for
140 repair of dsRNA by the undamaged strand (Tseng and Li 2005). Hence sequence data alone
141 theoretically implies that Φ6 inactivation goals should be similar to or slightly more conservative
142 than SARS-CoV-2. Separately, it is currently difficult to compare UV efficacy both within and
143 across different viruses based on existing data because experimental tests are highly variable
144 across different labs and studies (Hadi et al. 2020). Overall, the sequence comparison between
145 the two viruses is likely moot because debris, drying, and porosity of respiratory particles and/or
146 contaminated surfaces have dominant impacts on decontamination kinetics particularly when the
147 amount of debris is >99.999% relative to virus (United States Food and Drug Administration
148 2021; United States Environmental Protection Agency 2021). Furthermore, practical confidence
149 that test methods approach the challenge of field conditions is needed from field
150 decontamination testing in order to increase confidence in devices to be employed by end users
151 (Hamilton et al. 2013; Buhr et al. 2015, 2016).

152 Here Φ6 was prepared at 11.0 ±0.2 $\log_{10}$ PFU ml^{-1} without post-harvest processing or
153 concentration steps, and then dried on to different materials for >24 hours (h) to make BSL-1
154 live/dead enveloped virus test indicators at ≥ 8.0 $\log_{10}$ PFU $coupon^{-1}$. Numerous UV devices
155 were tested in both lab and field trials for both screening and iterative UV product improvement.
156 As a BSL-1 surrogate, Φ6 is useful for the generation of baseline decontamination data for
157 enveloped viruses, particularly during the COVID-19 pandemic when results from field
158 decontamination methods and procedures were urgently needed. It is recognized that the
159 limitation of Φ6 testing is that a correlation test with ≥5 independent batches of unpurified
160 mammalian coronavirus at ≥ 8.0 $\log_{10}$ PFU $coupon^{-1}$ is needed. The current limitation of such a
161 correlation test is linked to limitations with coronavirus preparation and test methods. COVID-
162 19 mucus is significantly thicker than healthy mucus (Kratochvil et al. 2022), but not yet defined
163 for virus inactivation testing. This natural microbial protectant will need standardized and
164 combined with virus to generate practical confidence for SARS-CoV-2 inactivation data. In
165 addition, titers of lab-prepared coronavirus needs to be significantly higher in order to meet the

166 virus load that has been measured and is expected in the environment. While there are
167 limitations in this study that center around the need for correlation testing with multiple,
168 independent batches of unpurified, >99.999%-debris (mucus) laden, dried coronavirus at ≥ 8.0
169 $\log_{10}$ per test, the Φ6 test met the quantitative, practical objectives, and was the most
170 conservative live/dead enveloped virus test known for field testing during COVID-19 and for
171 screening/selecting decontamination equipment and technologies (Buhr et al. 2020).

172

173 **MATERIALS AND METHODS**

174 **Φ6 and Host Cell Preparations**

175 Virus and host cell preparation was previously described (Buhr et al. 2020). Φ6 and its
176 host organism *P. syringae* pathovar *phaseolicola* HB10Y (HB10Y), causal agent of halo blight
177 of the common bean, *Phaseolus vulgaris*, were isolated in Spain. Both were a kind gift from Dr.
178 Leonard Mindich at Rutgers University, New Jersey Medical School. HB10Y was prepared by
179 inoculating 100-200 ml of 3% tryptic soy broth (TSB; Fluka PN#T8907-1KG) in a 1-liter (l)
180 smooth-bottom Erlenmeyer flask with a high efficiency particulate air (HEPA) filter cap.
181 Cultures were incubated at 26±2°C, 200 revolutions (rev) minute (min)$^{-1}$ for 20±2 h. 11.1 ml of
182 100% glycerol (Sigma PN #G7757-500ML) was added per 100 ml of host culture. Final
183 concentration of glycerol was 10%. One-ml aliquots of HB10Y were pipetted into screw-cap
184 microfuge tubes with O-rings and stored at -80°C. HB10Y samples were titered prior to freezing
185 by serially diluting samples in 10 millimolar (mM) of 4-(2-hydroxyethyl)-1-
186 piperazineethanesulfonic acid (HEPES, Sigma PN#H4034-100G) + 10% Sucrose (Sigma PN
187 #S7903-250G), pH 7.0, and plating on tryptic soy agar (TSA; Hardy Diagnostics, Santa Maria,
188 CA). Plates were inverted and incubated at 26±2°C for 48±2 h to show titers of ~10^9 cells ml^{-1}.
189 After freezing, tubes were thawed at room temperature (RT, 22±3°C), serially diluted, and plated
190 to show sustained viability after long-term storage at -80°C.

191 Φ6 was prepared after inoculating broth cultures of HB10Y. A frozen stock prep of
192 HB10Y was thawed at 22±3°C. HB10Y was added either directly from a frozen stock or by
193 transferring a single colony from a streaked TSA plate to 200 ml of 3% TSB in a 1-l smooth-
194 bottom Erlenmeyer flask with a HEPA cap and incubated at 26±2°C, 200 rev min^{-1} overnight.
195 Cells were then diluted and grown to mid-log-phase (3-5e8 cells ml^{-1}). The host flask was
196 inoculated with 0.5-1 ml of Φ6 at a stock concentration of 11±0.2 $\log_{10}$ PFU ml^{-1}. The culture
197 was incubated at 26±2°C, 200 rev min^{-1} for 24±2 h. The Φ6 preparation was stored at 4°C until
198 after titering was completed. After titer determination was completed, then 1-1.3 ml volumes
199 were aliquoted into 1.5-ml screw-cap tubes with O-rings, inverted, and stored at -80°C.

200 **Coupon Materials and Sterilization**

201 2 centimeter (cm) x 2 cm coupons of different test materials were inoculated with ≥8.0
202 $\log_{10}$ PFU Φ6 virus inoculum (Buhr et al. 2020). Materials for inoculation included stainless
203 steel 304 (SS304) (20 gauge with a 2B finish from Cardinal Scientific), SS304 coupons painted
204 with Navy Top Coat (NTC) (26 gauge SS304 with a 2B finish primed with N-6237 and top
205 coated with MIL-PRF-24635B, 4-6 mils from Coatings Group at the University of Dayton

206 Research Institute (Dayton, OH, USA)), acrylonitrile butadiene styrene (ABS) plastic (flat black
207 coupon from Cardinal Scientific), polymethyl methacrylate (PMMA) plastic (keyboard keys
208 from Hewlett-Packard computer keyboards), polyurethane (clear polyurethane national stock
209 number 9330-01-541-8524X3), and cardboard (hand-cut from a Corrugated Recycles, new,
210 single wall, cardboard box (Davis Core & PAD, Cave Spring, Ga, USA) with thickness of 0.16
211 inch). ABS and PMMA plastics are often used for computer keyboards. The plastics and SS304
212 represent non-porous materials. NTC represent semi-porous surfaces found on military ships.
213 Cardboard represents porous materials used in shipping although it is not as porous as fabrics or
214 carpeting.

215 For sterilization, SS304 and NTC coupons were rinsed with 18 mega-Ohm-cm, de-
216 ionized water, placed on absorbent paper in an autoclave-safe container, and autoclaved for 30
217 min at 121ºC, 100 kilopascals. PMMA keyboard keys were removed, trimmed, cleaned with
218 soap, then rinsed with de-ionized water, and wrapped in aluminum foil. ABS coupons were
219 similarly rinsed with de-ionized water and wrapped in foil. Cardboard coupons were devoid of
220 noticeable debris, flaws, and ink, and were wrapped in foil. After wrapping in foil, the PMMA
221 keyboard keys, ABS, and cardboard were all sterilized via hot, humid air at 95ºC and 90%
222 relative humidity (RH) for 4 h. Polyurethane coupons, having been pre-cut, were soaked in
223 ethanol to remove ink residue left over from the cutting process. They were then rinsed with de-
224 ionized water, sterilized via immersion in 70% ethanol for greater than 20 min, and allowed to
225 dry. All sterilized coupons were stored in sterile containers until used.

226 **Coupon Inoculation, Extraction, and Quantitation**

227 Five independent preparations of Φ6 were removed from -80°C storage and thawed at
228 22±3°C. Working inoculum was prepared by transferring stock Φ6 into 50-ml conical tubes
229 containing 10mM HEPES + 10% Sucrose pH 7.0 with a final concentration of ~9 $\log_{10}$ PFU ml^{-1}.
230 Coupons were inoculated with 0.1 ml of Φ6 working inoculum and subsequently held at 22±3°C
231 for greater than 24 h to dry and adhere to the material. The PMMA keyboard keys were slightly
232 slanted. Therefore, during inoculation and drying, the keys were positioned in a sterilized surface
233 which was elevated on an incline via slats to provide a level inoculation surface.

234 Once the inoculum had dried onto the coupons, they were exposed to UV from the
235 candidate devices. Specific parameters for testing the individual devices varied but coupon
236 number and preparation prior to testing was maintained across all experiments. For each test, five
237 individual coupons were included for each of the test materials (SS304, cardboard, NTC,
238 polyurethane, and either PMMA plastic keyboard keys or ABS plastic). Each coupon was
239 inoculated with one of five independent virus preparations as described above. Extraction and
240 shipping control coupons (inoculated and transported to the testing sites but not exposed to UV
241 radiation) as well as negative control coupons not inoculated with virus were also included for
242 every experiment. Finally, the Φ6 virus inoculum used to prepare the coupons was maintained at
243 RT from the date of coupon inoculation through the test, and viral titer was measured at the
244 conclusion of test exposures for each experiment.

245 To increase confidence in decontamination results and to conservatively estimate
246 decontamination requirements for enveloped virus in its native state, enveloped virus test
247 coupons were prepared to be protected similar to a natural virus without interfering with the

248 virus assay. Thus, Φ6 virus was unpurified to maintain natural stabilization with host cell debris
249 and was diluted in a 10% sucrose solution to mimic the presence of carbohydrates in mucus
250 without inhibiting the decontamination assay (Brakke 1951; Malenovska 2014; Buhr et al. 2020;
251 Hadi et al. 2020; Stadnytskyi et al. 2020). In addition, enveloped virus was dried on coupons
252 prior to testing since SARS-CoV-2 respiratory particles evaporate within seconds to generate dry
253 particles, and drying on fomites is also historically documented as a route of infection for
254 enveloped virus (Fenn 2001; Malenovska 2014; Hadi et al. 2020; Stadnytskyi et al. 2020).

255 After UV exposure, virus was extracted from both test and control coupons (**Figure 1**)
256 and plated in <25 min using a Φ6 extraction and overlay procedure that was previously described
257 (Buhr et al. 2020). For Φ6 extraction from materials (coupons), 5 ml of 10mM HEPES + 10%
258 sucrose pH7 were added to each conical tube with a virus-inoculated coupon and vortexed for 2
259 min. After vortexing, 5 ml of HB10Y log-phase culture (confirmed with real-time Coulter
260 Multisizer analysis) were added and allowed to infect at RT for 15 min, followed by 2 min of
261 vortexing. Each sample was serially diluted, from -2 to -6, in 900 µl of 10 mM HEPES + 10%
262 sucrose pH7. For each Φ6 dilution, from -1 to -6, 200 µl were transferred into individual tubes
263 containing 200 µl log-phase HB10Y. Then 200 µl of those Φ6/HB10Y mixtures were added to
264 individual TSB overlay tubes, poured onto individual TSA plates, and allowed to solidify for ≥30
265 min. Additionally, 1,000 µl was transferred from the 50 ml sample conical tube directly to a TSB
266 overlay tube, and the remaining 8.3 ml was poured onto two TSA plates, and also allowed to
267 solidify for ≥30 min. Solidified plates were then inverted, incubated for 20+/-2 h at 26°C, and
268 quantified. Plates were incubated an additional 24 h, RT and quantified a final time.

269 Quantitation and calculations of survival were performed as previously described (Buhr
270 et al. 2020). An important difference between virus and prior spore quantitation is that virus and
271 spore inoculum dried on to coupons was stable. However, titers of virus controls stored in
272 solution were unstable and highly variable whereas spore controls were stable in solution.
273 Therefore, virus inoculation titers were defined as 100% extraction, or maximum recoverable
274 virus, and used to calculate extraction efficiency for each material.

275 Virus survival and $\log_{10}$ reduction were then quantified using ASTM standard practices
276 E3092 and E3178 except plaque forming units (PFU) replaced colony forming units (CFU). The
277 sample mean and sample standard deviations were calculated for each set of samples. The virus
278 inoculation titer adjusted for the volume and dilution difference served as the 100% recovery
279 reference value for calculating the virus survival after decontamination. The extraction
280 percentage was an arithmetic calculation not a $\log_{10}$ calculation. The extraction percentage was
281 calculated by dividing the total number of infectious virus (PFU) extracted from the virus-
282 inoculated control coupons for each material type by the total number of inoculated virus (PFU)
283 (divided by 100 to adjust for 0.1 ml of viral inoculum deposited on each coupon and the 10 ml
284 extraction volume). An average extraction efficiency was calculated and recorded for each type
285 of test material for each test day. The number of surviving PFU for each test coupon was
286 corrected for extraction efficiency by dividing the number of surviving PFU by the extraction
287 percentage to determine the total number of PFU ml^{-1}. The virus survival of each test coupon
288 (corrected for extraction efficiency) in PFU ml^{-1} was multiplied by 10 to account for the 10 ml
289 total volume in each tube with extraction buffer. This gave the total number of surviving PFU
290 per sample. The virus survival of each control coupon in PFU ml^{-1} was also multiplied by 10 to
291 account for the 10 ml of extraction volume. Each number was converted to $1\log_{10}$. Since the

292 $\log_{10}$ of 0 is infinite and for simplicity, the number '1' was added to each number prior to
293 converting to $\log_{10}$. The $\log_{10}$ mean and $\log_{10}$ standard deviation was calculated for infectious
294 virus for each coupon material. The $\log_{10}$ reduction mean and standard deviation was calculated
295 for each coupon material. For the $\log_{10}$ reduction, the $\log_{10}$ mean of each coupon material was
296 subtracted from the $\log_{10}$ mean of the virus titer (minus 1 to adjust for 0.1 ml of viral inoculum
297 deposited on to each coupon), the 100% recovery reference value. For the $\log_{10}$ reduction
298 standard deviation, the square root of the result of the $\log_{10}$ survival standard deviation was
299 taken for each coupon squared; divided by the number of independent samples plus the $\log_{10}$
300 survival standard deviation of the virus inoculum titer squared; divided by the number of
301 independent samples.

302

303

304 **Figure 1.** Φ6 extraction procedure for test samples and non-treated controls.

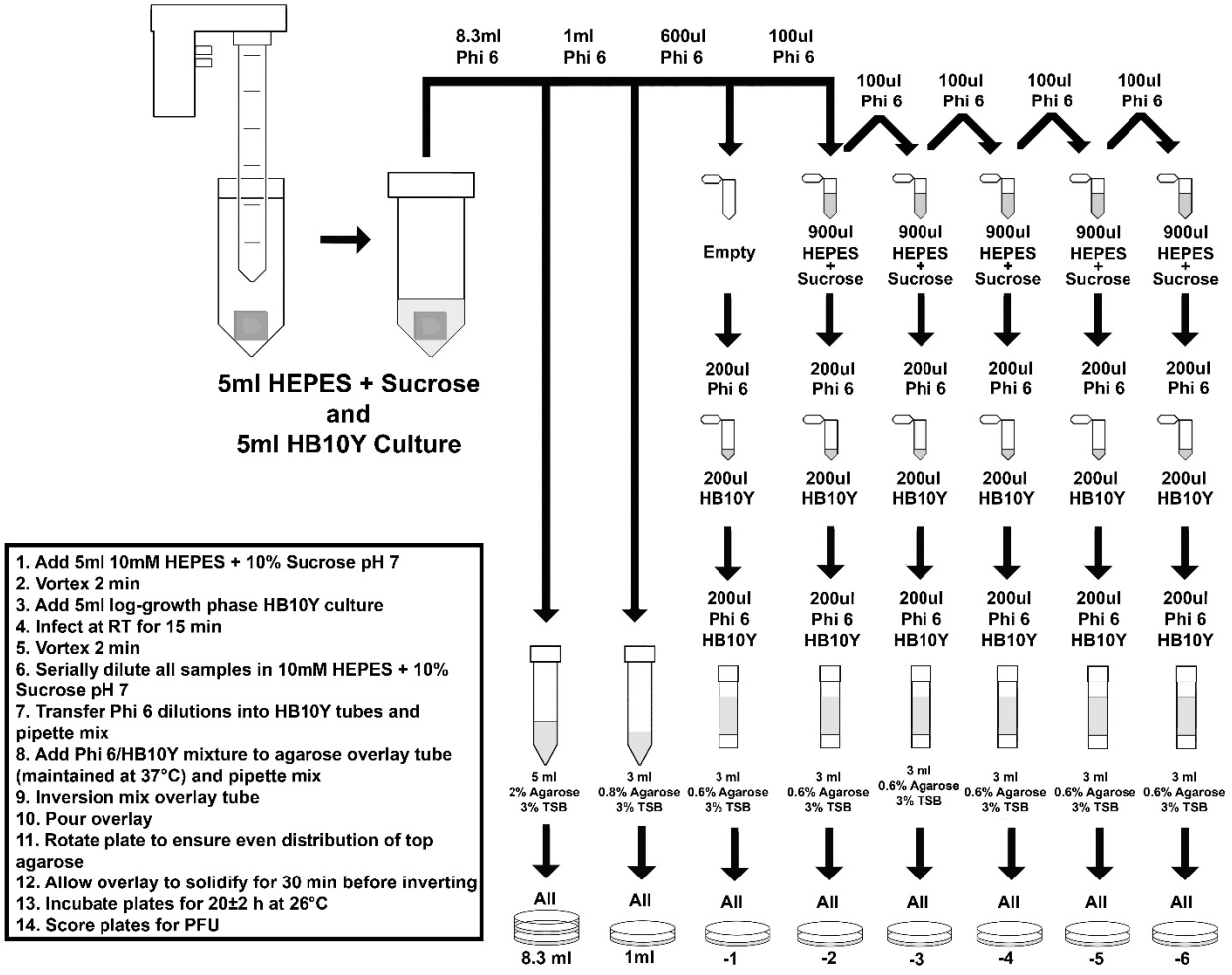

305

306

Spectroscopic Analysis Hardware and Calibration

The primary spectrometer used for this work was the Ocean Optics Maya 2000 Pro, which measured optical spectra from 180 – 630 nm with an average bin size of 0.22 nm across the measurable spectrum. The distribution is not strictly linear, but can be specifically determined as necessary for data processing. The spectrometer was used with a fiber bundle (BFL200HS02), which incorporates seven Φ200-µm core fibers into a single high-OH package. This enables the measurement of sources with low output so the spectrometer can both retain a high signal-to-noise ratio and enable the use of a cosine corrector (CCSA2) for most measurements.

The Maya 2000 Pro spectrometer was calibrated using a Cathodeon R48 Deuterium Lamp, serial number CH5627. The spectral irradiance from this lamp is in units of $mW \bullet m^{-2} \bullet nm^{-1}$ in 5 nm intervals from 200–400 nm. To perform the calibration, the lamp is mounted vertically and positioned so that a horizontal line through the center of the area to be irradiated passes through the center of the lamp emission area, as well as perpendicular to the lamp window. The calibration refers to the spectral irradiance over an approximately 10 mm^2 area in a vertical plane located at a distance of 200 mm from the outside surface of the output window on the lamp. The lamp is operated from a 300-mA power supply and must be operated continuously for 30 min prior to recording data on the spectrometer.

The spectrometer was mounted on an optical table, with a three-axis linear translation stage (Thorlabs LTS300) used to enable precision alignment between the spectrometer fiber sensor head and the source of interest. The three-axis system is capable of measuring a 300 mm x 300 mm x 300 mm volume with computer automation using a process-controlled script via the Thorlabs Kinesis software. The data acquisition software used National Instruments LabVIEW for all aspects except direct control of the translation stages. All of the data was written to a single Technical Data Management Streaming data file for post-processing, which enabled all of the measurements to have a common time base for analysis. Post-processing was accomplished with the Jupyter software environment with discrete Python code blocks to allow for processing of specific sources as needed. The raw TDMS data file is loaded into a cache file on the processing server, and a series of factors and calibrations are applied to prepare the raw data for analysis. Static measurements are relatively simple, as the position is fixed and no further analysis is required. Sweeps in a two-dimensional space with the translation stages requires synchronization of the position with digital fiducial markers to construct an image of the measured plane at a given distance from the source.

RESULTS

A focus of this work was to generate information for screening field devices and to provide feedback for iterative product improvement. Some data for prototypes were deliberately omitted since all prototypes were in the process of iterative improvement. The variability of UV emission from different test bulbs and devices (**Figure 2)** was enough by itself to justify the need for high confidence, quantitative, field test standards to guide product screening and iterative improvements in UV devices. Differences in intensity, dosages and virucidal efficacy among devices were additional justifications for standardized field testing described later.

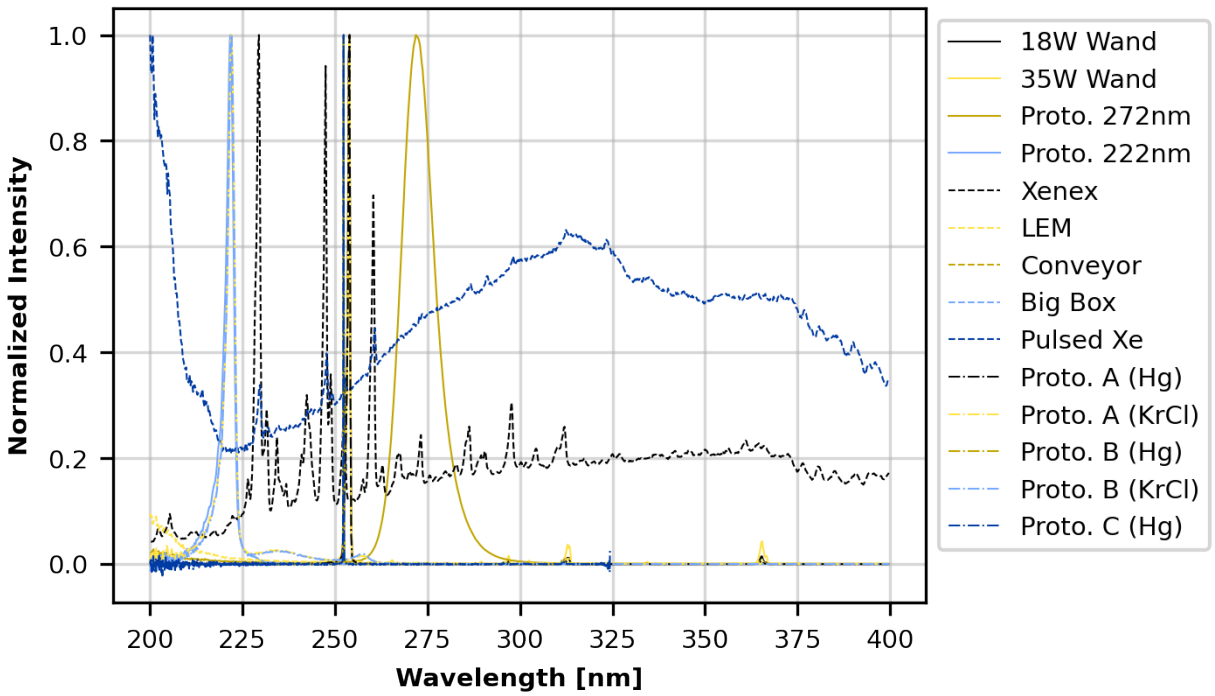

Figure 2. Normalized wavelength emission spectra for four handheld devices (18 watt wand (solid black line); 35 watt wand (solid light gold); 272 nm prototype (solid dark gold); 222 nm prototype (solid light blue)), five room devices (Xenex (dashed black); LEM (dashed light gold); medium conveyer (dashed dark gold); big box (dashed light blue); pulsed Xe (dashed dark blue), and five prototype devices (prototype A - Hg (dot-dashed black)); prototype A - KrCl (dot-dashed light gold); prototype B - Hg (dot-dashed dark gold); prototype B - KrCl (dot-dashed light blue); prototype C (dot-dashed dark blue)).

Extraction of viable virus from each non-treated control sample demonstrated that extraction efficiency was consistent across materials for 4-14 days (d) after coupon inoculation with >8 $\log_{10}$ virus and subsequent drying (**Table 1**). This was an important goal to meet in order to demonstrate that the method could generate reproducible results for tests at multiple field test sites outside of laboratory containment. The selection of materials to be inoculated for different devices was dependent on the intended use of different devices, the iteration of testing, and the availability of different materials, noting that different materials were available at different times during testing because of procurement limitations during COVID-19. After initial virus testing with keyboard keys, flat ABS coupons were procured. The keyboard keys were later identified as PMMA plastic rather than ABS plastic through Fourier Transform Infrared Spectroscopy, although both types of plastics are used for keyboards and both are non-porous, hard plastics.

372 **Table 1**. Average extraction efficiency of Φ6 virus 4-14 d after drying on different materials.

	PMMA Plastic	ABS Plastic	Cardboard	NTC	SS304	Polyurethane	Glass
Test Days	11	4	16	15	18	9	1
Total Samples	55	20	80	75	90	45	5
Extraction %	57.1±24.2	71.8±14.6	59.3±18.7	54.3±20.0	58.1±19.9	54.1±18.8	95.2±10.2

373

374

375 **Commercial handheld devices (18-watt, 35-watt)**

376 Two commercial handheld devices were acquired and tested, each within a custom test
377 apparatus. The first was the GermAwayUV 18W Handheld UV-C Surface Sanitizer (SKU
378 202110, bulb SKU 195317, CureUV, Delray Beach, FL, USA), a 120V/60Hz device containing
379 two 12.7-cm long, U-shaped (Hg) UV bulbs emitting 254 nm UV-C radiaton (**Figure 3A**). An
380 average intensity of 7.61 mW cm^{-2} was measured within a decontamination footprint of 4.47 cm
381 x 5.39 cm at a 5-cm standoff distance from the bulb (heat map of UV coverage is shown in
382 **Figure 3C)**. The second device was the GermAway UV Premier 35W Handheld UV-C Surface
383 Sanitizer (PN14-110-800-100, EPA Product No. 94850-DV-6, CureUV, Delray Beach, FL,
384 USA), 120V/60Hz handheld containing two Hg bulbs that emit 254 nm UV-C radiation, with
385 reflective material positioned within the unit to enhance UV coverage (**Figure 3B**). The twin
386 tube bulbs spanned a length of 22.5 cm. The 35W device provided an average intensity of 6.95
387 mW cm^{-2} at 5-cm standoff distance from the bulb (**Figure 3D**). The 35W handheld was later
388 discovered to contain ineffective ballasts (P/N 14-110-800-100), which negatively impacted
389 results.

390 For testing the two handheld devices, wooden holding chambers were constructed in
391 which the devices could be placed to provide standardized exposures to test materials. They were
392 designed to hold the UV source 5 cm above the surface of a test coupon, to prevent UV
393 reflection, and to allow coupons to be inserted into the apparatus via a sliding tray for a specified
394 time period of virus inactivation and then promptly removed (**Figure 3A and 3B**). The design of
395 the chambers was the same for the two devices and only varied in size to accommodate the
396 different dimensions of each device. The handheld devices had variable UV output immediately
397 after turning them on. In order to generate consistent dosage for lab-to-lab testing, the devices
398 were powered on 30 min prior to testing and remained powered on for the duration of the test.
399 Cost and schedule limitations prevented a statistical test among multiple handhelds from
400 different manufacturing batches to assess the variability within and among devices and to
401 determine a minimum warm-up time for end users. The variability highlighted an important gap,
402 dosage monitoring in the field, which needs addressed for end users. To prevent potential
403 contamination, the test chambers and devices were wiped down with pH6.8-adjusted bleach prior
404 to being positioned inside a biosafety cabinet (BSC) for testing.

405

406

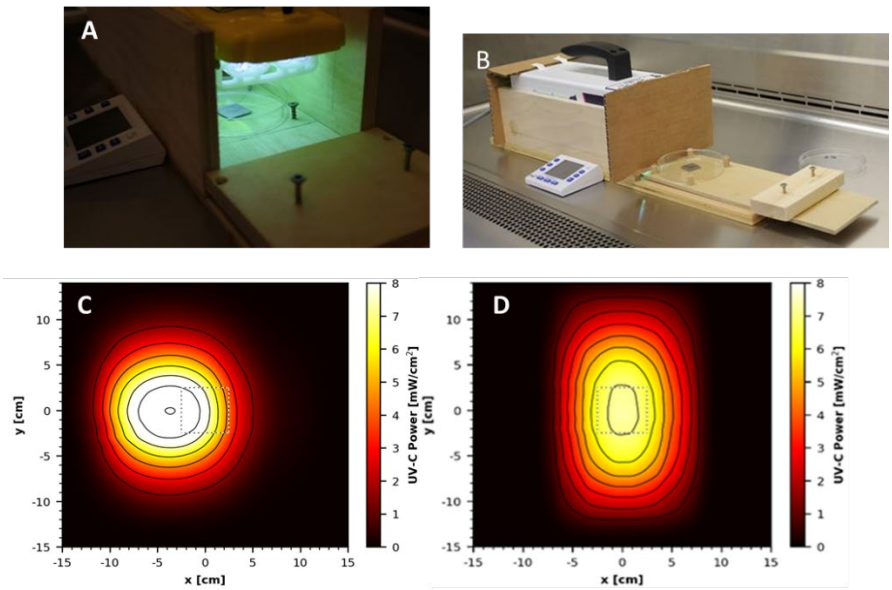

Figure 3. Testing setup and UV coverage for 18W and 35W handheld devices. **(A)** GermAwayUV 18W handheld device and custom test chamber, shown during a coupon exposure. **(B)** GermAwayUV 35W handheld device and custom test chamber, shown in the pre/post exposure state. **(C)** and **(D)** UV coverage heat maps for the 18W device **(C)** and the 35W device **(D)** taken 5 cm from the source.

The sliding tray was constructed to hold a sterile Petri dish via guides and included a stop bar to ensure that the sample would be consistently positioned directly under the center of the UV source for maximum exposure. A cardboard barrier was placed over the opening of the chamber to prevent premature UV exposure onto test coupons when the materials were outside the test chamber. The plastic lid was removed from the Petri dish prior to UV exposure and the dish was wide enough that the dish edges did not impede UV transmission.

A N=5 was tested for each material at each time point. Each of the 5 coupons was inoculated with an independent virus preparation, emphasizing statistical accuracy over precision, and 3 separate exposures were tested for a total N=15. Test chambers held the UV source at a distance of 5 cm from the coupons, with the exception of keyboard keys. The keyboard keys were taller, and the distance from the UV bulb was 4.28-4.38 cm. The 18W and 35W handheld devices emitted steady state intensities of 10.12 mW cm^{-2} and 6.9 mW cm^{-2} respectively at the geometric center under the device. Test coupons were exposed to 10 or 20 seconds (s) of UV-C radiation from the 18W handheld and 2, 5, or 10 s of UV-C radiation from the 35W handheld. Different exposure times for the two devices were chosen based on pre-experimental predictions that were considered for practical application of the devices in a field setting. Prior to testing it was assumed that 35W radiation would exceed 18W and 10 s was a common time variable for both the 18W and 35W handhelds. During testing, the ambient environment was 22±2°C and 40% RH. The surface temperature within the test chamber reached 36°C under the 18W device and 48°C under the 35W device. Following UV exposure, coupons were transferred using sterile forceps to 50-ml conical tubes for extraction. The corresponding

435 virus-inoculated control coupons were left at ambient conditions during testing because prior
436 testing with Φ6 showed complete recovery/survival of >8 $\log_{10}$ of dried virus after treatment of
437 different surfaces at 55°C, 50% RH for 1 h (Buhr et al. 2020). Of note, wet virus was completely
438 killed at 55°C, 50% RH for 1 h (Buhr et al. 2020), an important data point that supported the
439 goal for testing dried virus as described in the introduction and discussion. Hence, the heat
440 (48°C) could have potentially impacted decontamination kinetics if the tests had used wet virus
441 instead of dried virus. The UV test parameters here were short duration (up to 10 s) and the
442 surface temperatures likely did not equilibrate much above ambient temperature. Importantly,
443 the high temperatures measured under these handhelds generates a practical risk for the end users
444 because it is not known if the heat generated might create a fire hazard if the lamps are left on for
445 extended periods. While 48°C was the highest temperature measured among any of the devices,
446 temperature measurements over extended run periods for multiple different handheld batches
447 would be needed for safety assessments prior to field use, and this task was outside of the testing
448 scope.

449 The dosage and virus inactivation results are summarized in **Tables 2** ($\log_{10}$ reduction)
450 and **3** ($\log_{10}$ survival). Dosages and virus inactivation were measured at a 5 cm distance, which
451 was considered a reasonable, practical distance for a handheld device used to scan over surfaces.
452 The keyboard keys were slightly taller and closer to the UV source. Thus, the dosage on the keys
453 was slightly greater than the other materials but no dosage calculations were made specifically
454 for those keys.

455 To evaluate the efficacy of the devices, a minimum of 3-$\log_{10}$ inactivation was targeted,
456 which is equivalent to a 99.9% reduction and corresponds to the current EPA requirements for
457 chemical disinfection. A 10 s exposure with the GermAway 18W unit failed to meet the ≥3 $\log_{10}$
458 inactivation threshold for all tested materials. A 20 s exposure successfully achieved a greater
459 than 3 $\log_{10}$ inactivation out of an 8.2 $\log_{10}$ virus challenge on SS304, NTC, keyboard keys, and
460 polyurethane but failed to meet the 3 $\log_{10}$ inactivation threshold on cardboard.

461 The GermAwayUV 35W handheld sanitizer failed to meet the ≥3 $\log_{10}$ inactivation
462 threshold out of an 8 $\log_{10}$ PFU virus challenge on all five materials for all three exposure
463 durations, achieving less than 2 $\log_{10}$ PFU inactivation. The GermAwayUV 35W handheld
464 sanitizer delivered lower dosage than the 18W handheld despite nearly double the power. Hence
465 there was no correlation between power and dosage/efficacy, and the importance of measuring
466 every device was apparent.

467
468
469 **Prototype Handheld devices (272 nm LED and 222 nm Lamp Modules)**

470 Two additional handheld devices were tested for efficacy of virus inactivation, which
471 were prototypes rather than commercial units. The first prototype was one of two custom 3-D
472 printed proprietary units and featured eight LED strips which emitted 272 nm wavelength UV-C
473 radiation. The face of the handheld was 320 mm x 100 mm with the LED strips covering 255
474 mm x 60 mm. An average intensity of 12.71 mW cm^{-2} was measured within a decontamination
475 footprint of 6 cm x 25.5 cm at 5 cm standoff distance from the bulb (**Figure 4A and 4B**). The
476 second prototype device utilized three 222 nm UV-C Excimer Lamp Modules installed into a

2.54 cm thick white plastic panel with power supply. It is important to note that this was strictly an early prototype undergoing iterative improvements, and the UV sources were spaced too far apart for a wand configuration. An average intensity of 1.54 mW cm^{-2} was measured at 5 cm standoff distance from an individual module (**Figure 5A and 5B**).

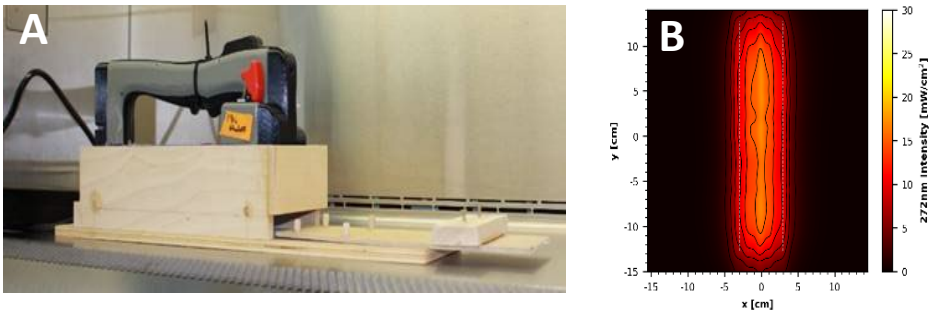

Figure 4. (A) Prototype 272 nm LED handheld inside wooden test chamber. **(B)** UV coverage heat map taken 5 cm from the source.

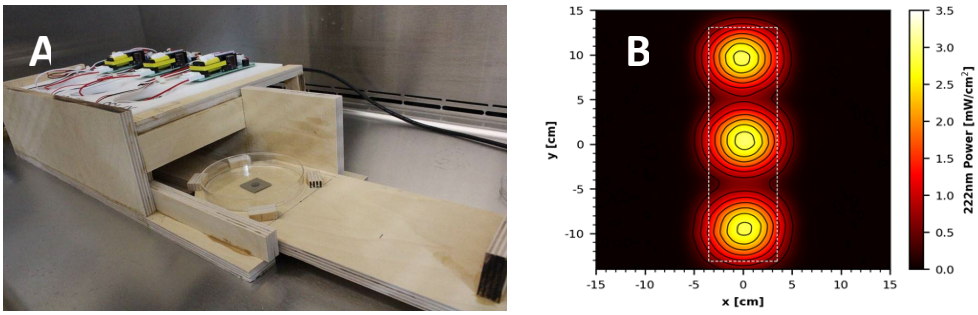

Figure 5. (A) Prototype 222 nm Excimer Lamp Module Board inside wooden test chamber. **(B)** UV coverage heat map taken 5 cm from the source.

The wooden test chambers for the prototype handhelds followed the same design as those for the 18W and 35W devices, with the additional feature of a wooden barrier that removed the need for cardboard to prevent premature UV exposure onto test coupons when the materials were outside the UV chamber. Again, there was a 5 cm vertical standoff distance from the UV source to the surface of the test coupons. Mimicking the 18W and 35W handheld unit tests, the devices were powered on 30 min prior to testing to warm up and remained powered on for the duration of the test. An Ophir Spiricon Starbright Dosimeter (S/N 949685, P/N 7201580) and sensor (S/N 954282, P/N 7Z02479) were used to confirm that the 222 nm device was on and emitting 222 nm UV radiation, as the design of the prototype did not allow visual confirmation that the device was on after it was plugged in. The test chambers and handheld UV devices were wiped down with pH6.8-adjusted bleach prior to being positioned inside a BSC for testing.

500 A N=5 coupons for each material were tested at each time/dosage with each coupon
501 inoculated with an independent virus preparation. During tests, virus-inoculated coupons were
502 transferred singly to sterile Petri plates and inserted into the test chambers via the sliding tray for
503 timed UV exposures at the geometric center of the handheld device. For the 272 nm device, the
504 cardboard coupons were anchored down using sterile pipette tips due to the large amount of air
505 movement generated by the cooling fans of the device. In the 272 nm prototype, coupons were
506 exposed to a steady state intensity of 15.6 mW cm^{-2} measured at the geometric center of the
507 device with a 5 cm standoff distance. Similarly, the 222 nm prototype emitted an intensity of
508 2.96 mW cm^{-2} at a similar location centered under a single lamp module. Following UV
509 exposure, the coupons were transferred to 50-ml conical tubes for extraction. For both devices,
510 test coupons were exposed to UV-C radiation for 2, 5, or 10 s. For the 272 nm device, the
511 ambient environment during testing was 21±2°C and 21% RH, and the surface temperature under
512 the sterilizer reached 34.7±2°C. For the 222 nm device, the ambient environment was 21.8±2°C
513 and 20% RH, and the surface temperature reached 28.3±2°C within the test chamber.

514 The dosage and virus inactivation results are summarized in **Tables 2** (log_{10} reduction)
515 and **3** (log_{10} survival). The 272 nm LED prototype successfully achieved a ≥3 log_{10} PFU
516 inactivation out of an 8.5 log_{10} PFU virus challenge for SS304 at 2, 5, and 10 s, for ABS at 5 and
517 10 s, and for NTC and polyurethane at 10 s. The hardest, smoothest material was SS304, and it
518 showed the greatest log_{10} reduction at all 3 time points. Cardboard showed the lowest
519 inactivation rate with no treatments providing ≥3 log_{10} PFU inactivation. Overall, the 272 nm
520 LED prototype showed significantly greater virus inactivation compared to the 18W and 35W
521 handheld commercial devices.

522 The 222 nm Excimer UV prototype failed to achieve a >3 log_{10} inactivation out of an 8.5
523 log_{10} virus challenge for all 5 materials tested, making it the least effective of the four handheld
524 devices tested. Further testing with longer exposure times might produce results passing the ≥3
525 log_{10} inactivation threshold. From a practical standpoint, this data showed that this 222 nm
526 prototype had poor efficacy and very limited utility. Since this was a prototype, iterative
527 improvements can be made to improve performance of this device.

528

529 **Prototype Mounted Pulsed Xenon Unit for Room Decontamination**

530 A prototype room-decontamination unit featuring a pulsed Xe UV bulb was tested. The
531 unit consists of a pulsed Xe bulb within a frame intended to be mounted onto a wall, ceiling, or
532 mobile tripod for room decontamination. The UV source emitted a small burst of broad-spectrum
533 radiation every 6 s with the burst lasting for a short duration. The electromagnetic spectrum
534 included UV-C, UV-B, UV-A, and violet-blue visible radiation. Reflector material was
535 positioned behind the source to enhance UV output.

536 Testing of the modified prototype took place within an enclosure provided by the vendor.
537 The device was mounted at 0.5, 1, and 2 m vertical standoff distance above the testing surface
538 (**Fig. 6**). Test coupons were placed below the prototype in sterile petri dishes and aseptic
539 technique was employed to the greatest extent possible while outside of a BSC to prevent
540 contamination. The coupons contained within Petri dishes were uncovered just prior to the test
541 and re-covered at the conclusion of the exposure times. Independent tests were run for 3
542 exposure times (15, 30, and 60 min), each taken at 0.5, 1, and 2 m distances from the UV source.
543 These time increments were determined via the recommended cycle lengths from the vendor and
544 corresponded to vendor test data (30 and 60 min only). The device was pre-programmed for 30
545 min run times, therefore for the 15-min increment, coupons were removed from the enclosure
546 without shutting off the device after 15 min had elapsed from the time of the first flash. For the
547 60-min cycle, two decontamination cycles were run sequentially.

548 Results for a mounted prototype containing a pulsed Xe bulb are shown in **Tables 2**
549 ($\log_{10}$ reduction) and **3** ($\log_{10}$ survival). This device emitted broad-spectrum radiation in pulses
550 occurring every 6 s with the duration of each pulse measured at 0.489 s, and the majority of the
551 dosage applied over the first few milliseconds of that time. Because of the broad spectrum
552 nature, the UV dosage could not be confidently measured. This device demonstrated measurable
553 efficacy at 0.5 m for 60 min, and the results were best on non-porous materials. Efficacy was
554 very limited at 1 and 2 m and shorter exposure times, particularly on porous cardboard, followed
555 by semi-porous NTC. As usual, the best efficacy was on the smooth surfaces: plastic and SS304.

556

557

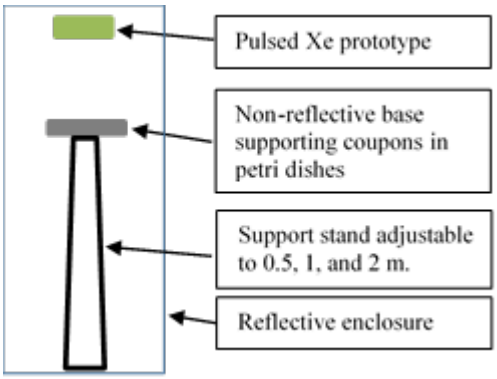

558

559 **Fig. 6**. Virus-inoculated coupons were placed 0.5, 1, or 2 m below the Pulsed Xe prototype.

560 **Commercial Rolling Units for Room Decontamination**

561 Two commercial rolling units designed for room decontamination were purchased. The
562 first was the Xenex Lightstrike (Model PXUV4D, S/N 002628, Xenex Disinfection Systems, San
563 Antonio, TX, USA), which contained one pulsed Xe bulb (broad spectrum across the germicidal
564 spectrum of 200-315 nm). The bulb extends and retracts at the top of the unit and pulsed at a
565 rate of 67 flashes per s. The intensities and dosages at specific wavelengths were not carefully
566 analyzed/dissected because the work was not aimed at correlating specific wavelength dosages
567 from a broad spectrum device to a kill rate. The second unit was the Light Emitting Module
568 ("LEM," Rapid UV-C Disinfection Model R3, S/N 473, 120V/12A, STERILIZ, LLC, 150
569 Linden Oaks, Rochester, NY 14625-2802), which contained a ring of twenty Hg bulbs with a 41-
570 cm diameter that emitted predominantly 254 nm wavelength UV-C radiation. The device was
571 tested at an exposure distance of 2.63 m from the center of the Hg bulb ring (**Fig. 7**). The length
572 of exposure was controlled based upon the cumulative dosage recorded via the LEM system
573 dosimeters placed next to the test coupons and targeted for exposures of 60, 100, and 140 mJ cm^{-}
574 ^{2}. Coupons were exposed to an average intensity calculated to be 0.23-0.24 mW cm^{-2}. Due to the
575 different expected intensities of the UV sources, the devices were set at different distances from
576 test coupons to achieve similar dosages in an attempt to directly compare the killing efficacy of a
577 broad spectrum radiation source to a 254 nm source.

578 For testing, the Xe or Hg rolling units were positioned in the corner of a triangular area
579 and non-reflective folding panels were set up to prevent UV exposure to personnel outside of the
580 decontamination area. Magnets were glued to the underside of test coupons prior to inoculation
581 of virus, and a black, non-reflective, metal sheet rack was utilized as a support for the test
582 coupons. The rack was bent into a curved shape in an attempt to maintain a constant UV
583 exposure distance to all coupons. Testing of these two devices required transport of coupons to
584 the testing site, and coupons were transported in 50-ml conical tubes at room temperature.
585 Negative control coupons as well as additional shipping controls (inoculated and transported, but
586 not exposed to UV) were also included. Conditions in the testing room were not aseptic but care
587 was taken to avoid contamination at each step and coupons were only transferred to and from the
588 metal rack using sterile forceps. After UV exposure, samples were transferred to new sterile
589 conical tubes and transported back to the microbiology lab for virus extraction and
590 quantification.

591 Specific testing conditions differed slightly between the two rolling units. For testing the
592 Xenex Lightstrike, the metal stand holding virus-inoculated test coupons was placed such that
593 the coupon height was between 1.09 and 1.55 m above the ground (approximately parallel to the
594 height of the pulsed Xe bulb), and the distance between the coupons and the UV source was
595 1.72-1.78 m. Based on preliminary dosage readings, the Xenex Lightstrike did not need a 30-min
596 warm up time. Two time points of 5 and 20 min were tested. Room conditions were measured at
597 23.3±1°C and 74% RH for the first exposure and 25.1±1°C and 22% RH for the second
598 exposure. As the tests occurred in succession approximately 30 min apart, the shift in
599 environmental conditions with the rise in temperature and drop in humidity is speculated to be
600 driven by the Xe unit itself. Additionally, the smell of ozone was detected in the air following the
601 completion of each test. Ozone level in the room was measured at 0.26 ppm for the Xenex
602 Lightstrike (0.1 ppm is the 8-h Occupational Safety and Health Assessment (OSHA) limit).

For testing the LEM, the metal stand holding virus-inoculated test coupons was placed such that the coupon height was approximately 1.2 m above the ground (parallel to center of the Hg bulbs), and the distance between the center of the ring of UV bulbs to the center of the metal arc with coupons was approximately 2.62 m. The distance between the test coupons and the nearest UV bulb was 2.43 m. Testing for this device included three independent exposures of 60, 100, and 140 mJ cm^{-2} which took 4 min 22 s, 7 min 2 s, and 9 min 33 s, respectively. The exposure conditions were 26±1°C, 38% RH. Ozone level in the room was measured at 0.08 ppm for the LEM (0.1 ppm is the 8-h Occupational Safety and Health Assessment (OSHA) limit).

Results for the Xenex Lightstrike unit with pulsed Xe UV bulb are shown in **Tables 2** and **3**. The Xenex Lightstrike failed to achieve a ≥3 $\log_{10}$ inactivation out of an 8.4 $\log_{10}$ PFU virus challenge for all 5 materials tested. A positive is that the Xenex did not require a warmup time in contrast to devices with Hg bulbs.

Results for the LEM with Hg bulbs are shown in **Tables 2** and **3**. The LEM successfully achieved a ≥3 $\log_{10}$ PFU inactivation out of an 8.4 $\log_{10}$ PFU virus challenge for SS304 at all three dosages, for polyurethane at the higher two exposures, and for NTC and keyboard keys at the highest dosage only. It failed to meet the ≥3 $\log_{10}$ PFU inactivation threshold for cardboard at all three exposure levels.

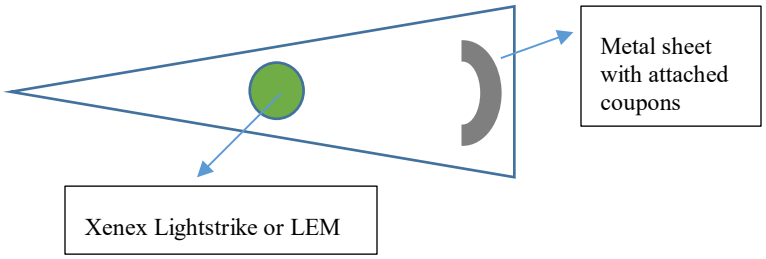

Fig. 7. Virus-inoculated coupons were placed 1.78 m horizontally from the Xenex Lightstrike or 2.63 m away from the LEM.

Prototype Medium Conveyer

The prototype medium conveyer featured a chamber measuring 2.03 m long x 0.78 m wide x 0.69 m tall that was lined on all interior surfaces with UV-C emitting (254 nm) Hg bulbs, including below the powered rollers (**Figure 8**). Testing of this device required transport of coupons to the testing site, and coupons were transported in 50-ml conical tubes at room temperature. Negative control coupons as well as additional shipping controls (inoculated and transported, but not exposed to UV) were also included.

Two rounds of testing were performed with the conveyer device, with slight differences in experimental setup and UV dosages. For both rounds, dosimeters were first used in trial-and-

error runs to determine the required run-through time to reach the target UV exposures. The dosimeters used were Roithner LaserTechnick GmbH GIVA-S12SD dosimeters from Vienna, Austria, with dimensions of 4.3 cm x 3.5 cm x 1.8 cm. In the first round of experiments, three dosimeters were horizontally taped to a 2% polyethylene board (46.7 cm x 28.6 cm x 2.54 cm) and were sent through the conveyor to get dosage readings based on exposure time (**Figure 8**). After target exposure times were determined, coupons were placed inside sterile Petri dishes and set on the same polyethylene support board before exposure in the conveyer. The first round of testing included exposures of 60 mJ cm^{-2} (22 s), 100 mJ cm^{-2} (32 s), and 140 mJ cm^{-2} (44 s). Conditions within the conveyer for this round were 27.7 °C, 63.2% RH, 0.09 ppm ozone.

In the second round of testing, the initial runs were again dosimeter-only to determine exposure times to reach the targeted UV dosages. The same dosimeters were used, but this time they were placed on a ceramic tile (~45.7 cm x 45.7 cm). During testing, coupons were placed directly on the ceramic tile support to prevent the sides of the Petri dishes from blocking any UV radiation from reaching the coupons. Test conditions were 17.3±1°C and 20.1% RH. Ozone reading was not captured since the ozone reader was unavailable.

Two rounds of testing were carried out for the prototype medium conveyer with Hg bulbs, with each round varying in dosages tested and in the method of exposing the test coupons. The dosages over time were not perfectly linear. The dosage variability over time might have been variability in dosimeter readings and/or variability in Hg bulb dosages after warmup. Test results are shown in **Tables 2** and **3**. During round 1 testing at 60 mJ cm^{-2} (20 s), 100 mJ cm^{-2} (32 s), and 140 mJ cm^{-2} (44 s), the conveyer successfully achieved a ≥3 log_{10} PFU inactivation out of an 8.2 log_{10} PFU virus challenge for all three exposure times on SS304, NTC, ABS plastic, and polyurethane, with slightly higher inactivation results for ABS plastic and polyurethane at the higher two treatments. It failed to meet the ≥3 log_{10} PFU inactivation threshold on cardboard for all three exposure times.

For round 2 of testing, the dosages measured during testing were 13.7 mJ cm^{-2} (8s), 23.8 mJ cm^{-2} (16s), 40.0 mJ cm^{-2} (24s), and 56.2 mJ cm^{-2} (32s). Regardless of dosage variability, the conveyer successfully achieved a ≥3 log_{10} inactivation out of an 8.4 log_{10} virus challenge for SS304 at 24 and 32 s, for NTC at 32 s, and for ABS plastic at 32 s time points. For all other materials and round 2 exposure times, it failed to reach the ≥3 log_{10} PFU threshold inactivation.

The conveyor produced UV dose-dependent inactivation at lower dosages (13.7-56.2 mJ cm^{-2}), but inactivation leveled off across all surfaces tested at higher dosages (60-140 mJ cm^{-2}). The size of the shielded virus population was dependent on material porosity since the highest level of inactivation was observed on non-porous SS304, followed by polyurethane, ABS plastic, NTC, and then porous cardboard. In addition, a sub-population of virus protected by debris was shielded from exposure to radiation because of the presence of host cell debris as indicated by a flattening of the kill rate across all the materials including smooth SS304. That sub-population of debris-complexed virus manifest may manifest higher resistance to the damaging effects of the UV radiation because of both shielding and drying; it is widely known that UV damage produces pyrimidine dimers in nucleic acid and biochemical reactions involving bond formation typically require a solvent like water.

Figure 8. Dosimeters traveling down conveyor to determine exposure times for target UV dosages.

Prototype Big Box UV Chamber for Pallets

A prototype Big Box UV Sterilizer, a proprietary UV-C decontamination device, was acquired for virus inactivation testing. The outside dimensions were 2.74 m x 2.24 m x 2.4 m with an interior large enough to accommodate a recommended maximum load with dimensions of 1.21 m wide x 1.21 m long x 1.52 m tall. Max interior load was 1,134 kg. The interior was lined on five surfaces with a total of 320 T8 Hg bulbs, each measuring 0.9 m long and emitting 254 nm UV-C radiation. A double-stacked pallet mock-up of dimensions 1.02 m x 1.22 m x 1.64 m was placed within the UV chamber (**Figure 9**), centered from left to right, and positioned up against the rear backstop on the base of the chamber.

During testing, coupons were placed in Petri dishes on top of the pallet in five separate locations with lids removed prior to exposure. The UV chamber doors were closed, and the chamber was operated via a pre-programmed cycle set to run for 2 min followed by a 30 s exhaust. After UV exposure, the coupons were recovered, and the surviving virus was extracted and quantified. There was a single combined 2 min exposure test run for all coupons except for ABS plastic coupons, which was tested for 2 min on a separate test day. Room temperature extraction control samples were transported to and from the test location along with test coupons. Peak ozone generated was 0.36 ppm. Ozone was purged out of the chamber top for 30 s prior to opening the doors.

Results for the prototype Big Box UV sterilizer are shown in summary **Tables 2** and **3**. A large double-stacked pallet mock-up was set inside the Big Box UV sterilizer. Coupons were then set on top of the plastic and cardboard mock-up for UV exposure, and the distance from virus-inoculated coupon to the nearest Hg bulbs on the chamber ceiling was 16.5 cm. The dosages varied significantly at different locations in the box resulting in a dosage range of 377-729 mJ cm^{-2} for the test materials. Virus inactivation test results after UV treatment of 8.4 log_{10} PFU of enveloped virus deposited per coupon (8.2 log_{10} PFU for ABS plastic) showed a $\geq$5 log_{10} PFU inactivation for SS304, polyurethane, and ABS plastic and a $\geq$3 log_{10} PFU inactivation for NTC and cardboard. As for all other devices, the hardest, smoothest material (SS304) was most effectively treated while the most porous material (cardboard) was hardest to decontaminate.

Overall, the prototype Big Box chamber showed higher virus inactivation compared to almost all other devices, corresponding to the significantly higher UV dosage achieved with the large number of Hg bulbs in the chamber. The data highlights the overall limitations of UV technology to provide complete virus inactivation since virus sterilization was not achieved despite a large, powerful system featuring a total of 320 Philips T8 Hg bulbs.

Figure 9. Prototype Big Box UV-C Chamber with a double stacked pallet (top). Coupon placement inside petri plates on top of pallet for testing (bottom).

722 **Prototype Fixed UV Devices for Room Decontamination**

723 Three prototype devices were also tested that were intended to be installed on the ceiling
724 or wall to provide viral decontamination of the air. These devices followed the same general
725 concept but differed slightly in design and were tested in iterations that featured different UV
726 radiation sources (Hg and KrCl bulbs). Test setup for these devices was largely similar to the
727 previous devices with each test being carried out for five coupons and each inoculated from one
728 of five independent viral preparations. Sterile control and extraction control coupons were also
729 included. However, only one coupon material was tested for each device. Because the purpose of
730 these devices is air decontamination, the specific test material employed here was not
731 particularly important so long as the material was non-porous with high extraction efficiency and
732 the materials provided no additional decontamination properties. SS304 was initially used for
733 testing and was later replaced by quartz glass in one case, as it allows greater UV transmittance
734 to maximize the surface area that would be exposed to UV, and is similar to the way air particles
735 would be exposed at all angles to direct or reflect UV. Testing virus-inoculated glass was a late
736 decision during testing that increased the likelihood of UV penetration from multiple angles in
737 order to prove that UV was able to kill the majority of an 8-$\log_{10}$ dried virus challenge. The
738 glass tests also provided time and distance data point that might be used in future iterations of
739 aerosol testing to calculate and predict air flow requirements for air decontamination. Tests were
740 carried out for 5, 10, and 15 s for each device, though the distance from the UV source differed
741 for each device as described below. For all experiments, the devices were powered on for at least
742 30 min prior to testing to mitigate any start-up fluctuations in UV output.

743 Devices intended for air decontamination represent a challenge because methods to
744 mimic respiratory enveloped virus for field testing (testing outside of laboratory containment),
745 with a testing turnaround time of 2-weeks , have yet to be developed. While there are
746 nebulization protocols for wet purified virus in laboratory testing, these methods have little
747 practical relevance for field testing of environmentally relevant SARS-CoV-2 virus where the
748 virus is protected by mucus (the surface of which primarily consists of carbohydrate), the
749 infectious particles only consist of ≤0.001% virus, and the infectious 4 um particles are dry, not
750 wet (Hadi et al. 2020; Stadnytskyi et al. 2020). Lab testing of virus suspended in solution
751 demonstrated that virus would not reproducibly survive shipping for field tests (Buhr et al.
752 2020). For the purposes of this work, the methods for field testing on virus-inoculated surfaces
753 were maintained in order to comparatively screen and assess the effectiveness of the UV bulbs
754 used in the different prototypes, particularly since there was so much variability in dosage and
755 efficacy among different UV sources up to this point. This approach helped with iterative
756 assessments and prototype improvements.

757 **Prototype Device A (Hg bulb and KrCl bulb iterations)**

758 Prototype device A featured an internal UV source within an enclosed chamber. Fans
759 controlled flow into the chamber where air was exposed to UV-C radiation and then exhausted
760 through vents opposite from the fans. The first prototype contained two Philips TUV 15W/G15
761 T8 mercury bulbs emitting 254 nm UV-C. Three fans were mounted in the device to provide
762 airflow at 3,030 l min^{-1} total through an effective inner volume of 24.64 l. This led to a residence
763 time of 0.49 s that air would be exposed to UV radiation within the upper chamber. Exposures
764 were at 5 cm, 10 cm, and 15 cm from the UV source.

765 The second iteration of device A replaced the dual Hg bulb with a single, custom KrCl
766 excimer bulb from Far-UV Sterilay that emitted 222 nm UV-C, with the goal of developing a
767 device with good decontamination efficacy that also posed less of a hazard to personnel exposed
768 to the UV source. The modified prototype A unit was determined to require approximately 5 min
769 for the UV-C output to stabilize. The device was verified to emit a peak wavelength of 222 nm
770 with a slight spike at 252 nm likely from the SiO_2 glass casing of the bulb (data not shown). The
771 modified device A also included Teflon reflective surfaces to resist dirt build-up and provide
772 reflectance of the UV-C. High purity non-crystalline-fused silica glass plates, also called quartz
773 glass, were added to channel airflow parallel to the UV-C source and increase the total contact
774 time between contaminated air and the UV-C. This increased the total UV dosage applied to air
775 in the unit, thereby providing greater efficacy. The modified prototype device featured three fans
776 providing 1,700 l min^{-1} of airflow each into the unit. One fan was always operated with the UV-
777 C power switch. Two additional power switches were present for each additional fan, therefore,
778 the device could operate at 1,700, 3,400, and 5,100 l min^{-1} airflow. The effective interior volume
779 was 24.33 l.

780 The efficacy of the UV source within the modified device A (KrCl bulb) was tested with
781 the lid attached. Inoculated quartz glass test coupons were placed individually into a tray and slid
782 inside the unit through slots cut in the frame. Slots were cut at set distances of 4, 10, and 20 cm
783 from the center of the UV bulb. These distances were aligned to prominent design features in the
784 box. The 4 cm test distance (4 cm from the center of the bulb or 2 cm from the edge of the bulb)
785 aligned to an average distance from the bulb in the middle or second air flow channel. The 10 cm
786 distance aligned to the outer channels just behind the quartz glass, and the 20 cm distance also
787 aligned to the outer channels behind the glass at the furthest distance within the device where air
788 would be exposed to UV-C.

789 **Prototype Device B (Hg bulb and KrCl bulb iterations)**

790 Prototype device B featured a single UV-C source in an open-ended unit. Fans directed
791 airflow into the underside of the unit, and air then exited the frame under and past the UV-C
792 source and then out into the surrounding room air. As with device A, two iterations of the design
793 were tested. The first iteration contained one Philips TUV PL-L 36W/4P Hg bulb. Device B was
794 designed to be mounted to a wall and featured one fan to draw air upwards from underneath the
795 device and exhaust out the top and upper sides. It required a mounting height of 2.15 m in order
796 to ensure that no humans or pets are exposed to the UV-C coming out the sides of the device.
797 Test exposures for this device were conducted at 5 cm, 10 cm, and 15 cm from the UV source.
798 Coupons were placed in plastic Petri dishes with lids removed for exposures.

799 The second version of device B contained one KrCl excimer bulb emitting 222 nm UV-
800 C, the same bulb as in the second iteration of device A. With replacement of the 254 nm Hg bulb
801 with 222 nm UV emission, it no longer had the strict requirement of a 2.15 m mounting distance,
802 according to the prototype developer. However, 222 nm UV exposure was still a concern for
803 Navy personnel. Device B contained limited Teflon as a reflective surface was placed near the
804 bulb to direct and concentrate UV outward. Unlike device A, device B does not feature a closed
805 compartment where reflectivity with the Teflon can occur (substantially removing that potential
806 for an increase in applied dosage). The device featured a recessed UV compartment between 10-
807 15 cm deep with cross sectional area 38.7 cm x 11.4 cm. The compartment was angled upward

808 at approximately 45° from vertical to exhaust air and provide continuous UV exposure of
809 ambient air. The average measured airflow at the compartment outlet was 2,237 l min^{-1}. Test
810 exposures for this device were conducted at 5, 15, and 30.5, 61 and 122 cm from the UV source.
811 Coupons were placed in plastic Petri dishes with lids removed for exposures.

812 **Prototype Device C (Hg bulb type only)**

813 Prototype device C followed a similar concept to device B but with a slightly different
814 configuration and form factor. It was designed to be mounted to a wall and featured one Philips
815 TUV 36W/G36 T8 Hg bulb and two internal fans, with the fans placed to draw air upwards
816 through the unit to exhaust out the top and upper sides. Like device B, it requires a mounting
817 height of 2.15 m in order to ensure that no humans or pets are exposed to the UV-C coming out
818 the upper sides of the device. Test exposures for this device were conducted at 5, 10 and 15 cm
819 from the UV source. Coupons were placed in plastic Petri dishes with lids removed for
820 exposures.

821 **Mounted Prototypes A, B (Hg bulb and KrCl bulb prototypes), and C (Hg bulb type only)**
822 **Efficacy**

823 Efficacy results for the mounted prototype A, B and C are shown in **Tables 4** (log_{10}
824 reduction) and **5** (log_{10} survival). Prototypes were tested at representative exposure distances,
825 but the exposure times were much longer than expected for application in order to provide
826 modeling data. Bio-efficacy testing on the original prototypes A, B, and C evaluated the
827 performance of the UV source only. Testing on the modified prototypes A and B evaluated the
828 internal improvements to the device. Thus, bio-efficacy data presented would be significantly
829 less if realistic, shorter times were tested. For the original prototype A with the Hg bulbs, there
830 was minimal log_{10} reduction at different distances and times against virus-inoculated SS304. A
831 modified prototype version with a greatly optimized internal configuration and a KrCl bulb was
832 tested against virus-inoculated quartz glass. Time and cost restrictions prevented a test on virus-
833 inoculated SS304. This modified prototype A unit showed a significant improvement over the
834 original prototype. There were too many significant changes between the first and second
835 prototypes to isolate any single variable as the primary reason for the improved efficacy.

836 For the original prototype B with a Hg bulb, there was minimal log_{10} reduction at
837 different distances and times against virus-inoculated SS304. A modified prototype B with a
838 KrCl bulb emitting 222 nm UV was tested. Test results showed worse efficacy results than the
839 original prototype B. Overall, this device was the least effective of the wall-mounted prototypes,
840 and it was not modified as extensively compared to the modified prototype A. The 222 nm KrCl
841 bulb clearly did not improve efficacy in this prototype.

842 Prototype C had the least favorable design, and given its low efficacy, it was not pursued for
843 modification.

844
845

846 **DISCUSSION**

847 The focus of this research was to establish reference field test methods for UV
848 decontamination of enveloped virus and to both assess and accelerate improvements in UV
849 devices. Φ6 was selected as a BSL-1, enveloped RNA virus test indicator for both lab and field
850 tests. Φ6 has been widely used as an enveloped virus surrogate (de Carvalgo et al. 2017). It
851 bears structural similarity to many other enveloped viruses including coronaviruses, suggesting
852 that the Φ6 structure should be similarly susceptible to general decontaminants. The structural
853 molecules of the virus are produced by host cells with temperature sensitivity at around 40°C,
854 further suggesting that Φ6 should be similarly susceptible to general decontaminants as animal
855 coronaviruses. The capabilities for measuring UV efficacy using both physics-based equipment
856 and live, enveloped virus test indicators allowed standardized test measurements in both lab and
857 field tests to directly compare the different UV devices.

858 Greater than 1,000 Φ6 test samples, plus the corresponding Φ6-inoculated, non-treated
859 coupon controls and inoculum controls, were decontamination tested with ≥8 $\log_{10}$ Φ6 sample^{-1}
860 during COVID-19 in both lab and field testing (>20 field tests), which included both hot, humid
861 air (Buhr et al. 2020) and this UV testing. A total of 20 independent Φ6 preparations with a titer
862 of 11±0.2 $\log_{10}$ were generated on different days by 13 different technicians. Five independent
863 virus preparations were tested on each material for each test. A total of 13 technicians were
864 interchangeably used in different steps of the virus quantitation procedure, and 9 technicians
865 were used on a standard high throughput test day. The reproducibility of the test controls across
866 different test days with numerous technicians and with virus extraction that ranged from 4-14 d
867 after inoculation demonstrated reproducibility of the test method. Methods reproducibility in
868 this data set was critical because coronavirus test methods and results varied significantly during
869 COVID-19, which limited the confidence with which to interpret most published data on
870 coronavirus stability and decontamination (Hadi et al. 2020). Furthermore, critical
871 characterization data needed for accurate and relevant SARS-CoV-2 inactivation testing, such as
872 COVID-19 mucus characterization (Kratochvil et al. 2022), are only now beginning to get
873 published.

874 Enveloped virus stability had been confirmed previously; purified virus was unstable, but
875 unpurified virus was stable and could be stored dried onto coupons for at least 2 weeks prior to
876 extraction (Buhr et al. 2020). The instability of enveloped virus in solution is a key difference
877 compared to spore quantitation because spores are stable in non-nutrient aqueous solution at
878 temperatures up to at least 65°C. Hence, wet spores can be stored at room temperature for many
879 days alongside inoculated coupons (Buhr et al. 2012), whereas enveloped virus stored at ambient
880 temperature was only stable after drying (Buhr et al. 2020). Furthermore, there was no Φ6
881 inactivation after unpurified virus was dried onto different surfaces and incubated for a 10 d
882 exposure to 26.7°C at 80% RH, and only 2.4 $\log_{10}$ inactivation was seen after treatment at 70°C,
883 5% RH for 24 h (Buhr et al 2020). More work will be needed to confirm that Φ6 and BSL-2/3
884 coronaviruses are stabilized similarly in the presence of carbohydrates and mucus, and after
885 drying, but the first challenge is to generate sufficient BSL-2/3 coronavirus to match the titers
886 (and statistical confidence) of the Φ6 tests. This goal has not yet been met. In addition, neither
887 SARS-CoV-2 nor BSL-2 virus field testing is likely to happen with regularity.

888 The field testing in this manuscript is part of an iterative process of testing, test methods
889 development, and UV analysis. These test methods serve as a baseline screening for military end
890 users, military applications, and for military-relevant environments. To assess manufacturer
891 claims of UV decontamination, different UV bulbs were directly tested with a live/dead
892 enveloped virus assay at >8 $\log_{10}$ per test sample with 5 independent virus preps per test material
893 and the virus was dried >24 h prior to testing. Furthermore >50% of inoculated virus was
894 extracted from different control materials for up to 14 d after inoculation and showed to be "live"
895 in a live/dead assay. These controls were needed to validate field test samples. In order to
896 generate confidence and approve a device for end user fielding, additional testing of aerosolized
897 virus will need to be matured. Correlation tests among BSL-1, 2 and 3 enveloped virus will need
898 completed, and then tests will also need to be conducted inside buildings, ships, and aircraft to
899 adjust for variations in air movement and various power outages among all those
900 locations. There will be no lab containment for field testing, so a live/dead assay using a BSL-1
901 organism will be needed for those tests. As described in the introduction, virus particles will
902 need to be >99.999% non-volatile components, potentially including mucus for a respiratory
903 virus where human airway mucus contains 75-90% carbohydrates (Hadi et al. 2020). Here the
904 assay was simplified using >99.999% sucrose because sucrose is a carbohydrate with
905 representative carbohydrate hydroxyls found on the surface of mucin, a glycoprotein critical to
906 the function of mucus, and because there was not sufficient data to define mucus and drying
907 methods for coronavirus-relevant field testing during COVID-19. Furthermore, sucrose is a
908 known stabilizer that has been historically used for virus purification, and it was empirically
909 determined during Φ6 methods development to positively impact the Φ6 plaque assay (Brakke
910 1951, 1967; Buhr et al. 2020). Sugars and amino acids also absorb some UV radiation (Uchiho
911 et al. 2015) that partially protects virus in the environment, and this was a secondary benefit to
912 increase confidence in the field test results since mucin is composed of sugars and amino acids.

913 This UV work was aimed at directly assessing claims that UV radiation would kill
914 enveloped virus using a high confidence live/dead virus assay (≥8 $\log_{10}$ of dried virus with virus
915 controls that were recoverable out to at least 2 weeks). Aerosol testing is another layer of testing
916 that will be useful for UV decontamination screening. It is more complex because additional
917 variables such as air movement need controlled and high virus titers are needed in order to
918 generate confidence that the data will represent environmental virus loads. Aerosol testing
919 described in ASTM standard practice E2721-16 was a critical step forward for aerosol testing of
920 wet-dispersed viruses particularly influenza H1N1, and it described one potential artificial saliva
921 recipe that can be added to virus samples (Heimbuch 2013, Anonymous – ASTM 2016). The
922 healthy saliva option contains 0.3% mucin and a total of ~0.6% non-volatiles, but the ASTM
923 standard practice is flexible and not restricted to that option. This is important because a
924 considerable amount of data describing mucus over the past decade was published after ASTM
925 standard practice E2721-16. Saliva/oral fluids contain mucin glycoprotein, electrolytes, proteins,
926 DNA, lipids, and host cell debris: remnants of dehydrated epithelial and white blood cells
927 (Williams et al. 2006; Lai et al. 2009; Vejerano and Marr 2018; Hadi et al. 2020). Mucin
928 glycoproteins are critical to the function of mucus (Lai et al. 2009), and there are over 20
929 different types of mucin in humans (Corfield 2015). Similar to sucrose, hydroxyl groups on
930 mucin glycans control water activity (Znamenskaya et al. 2012). Unlike sucrose, the glycan
931 subunits on different mucins are variable, which creates variability in water activity as it pertains
932 to mucin resuspension from dried, commercial sources, and in mucin gel formation
933 (Znamenskaya et al. 2012). Hence, selection of sucrose for field testing during COVID-19 was a

934 simple, homogenous replacement that was easy to standardize for the live/dead screening tests
935 conducted early during COVID-19.

936 Commercially, two common animal mucins are readily available and frequently used:
937 porcine gastric mucin (PGM) and bovine submaxillary mucin (BSM). PGM is sourced from
938 intestinal epithelium and is desired in experiments due to its sialic acid content that best matches
939 respiratory mucins. BSM is sourced from submaxillary glands in the floor of a cow's mouth.
940 While mucin is a major element of saliva, another component of saliva than can interact with
941 mucin is a lung surfactant which is made up of about 90% phospholipids and 10% proteins
942 (Bredberg et al. 2012). The most abundant and active phospholipid in respiratory droplets is
943 dipalmitoylphosphatidylcholine (DPPC) (Niazi et al. 2021). A DPPC saliva recipe (0.9%,
944 sodium chloride, 0.3% porcine gastric mucin, and 0.05% DPPC) was mixed with Φ6, as an
945 enveloped virus surrogate for H1N1, and DPPC protected the mucin to prevent gel formation
946 (Vejerano and Marr 2018). Thus, saliva phospholipids are another potentially important
947 ingredient that might be added to mucus recipes for future iterations of decontamination testing.

948 The impact of drying on virus stability was a similarly important topic as it is known that
949 enveloped viruses are stabilized by drying (Cox and Wathes, 1995), and SARS-CoV-2 virus has
950 been shown to survive for up to 4 weeks after drying on materials (Riddell et al. 2020). Drying
951 for >24 h was a practical requirement for field testing in this work since samples were routinely
952 shipped to and from test sites. Future aerosol field tests would likely require virus release and
953 monitoring over time, which is beyond the current scope of existing test methods. Defining a
954 final quantity of non-volatiles to generate a standardized mucus solution to mix with enveloped
955 virus is further complicated by the prospect that respiratory disease-afflicted individuals may
956 produce a thicker and/or dryer mucus during different stages of illness as compared to healthy
957 persons (Vejerano and Marr 2018; Kratochvil et al. 2022). Coronavirus particle measurements
958 in 2020 indicated that 12-21 um speech particles would dry to 4 um particles in seconds and
959 smaller particles <1 um in size have such a small probability of containing virus that such a size
960 is likely negligible for infection (Stadnytskyi et al. 2020). A volume/volume calculation
961 indicates that the 12-21 um particles would contain 0.8-3.7% non-volatiles to generate ~4 um
962 dried particles. Assuming a worst case scenario where the highest level of non-volatiles is
963 protecting enveloped virus, then a mucus recipe with 3.7% non-volatiles contains about 3-6x
964 more non-volatiles compared to existing mucus recipes with 0.6-1.25% total non-volatiles (Aps
965 and Marten 2005; Heimbuch et al. 2013; Anonymous – ASTM 2016; Vejerano and Marr 2018).
966 COVID-19 mucus characterization was recently published showing a mean load of ~4.7% solids,
967 and significantly higher amounts of mucin glycoprotein and DNA compared to healthy samples
968 (Kratochvil et al. 2022). The characterization data for COVID-19 mucus non-volatile
969 ingredients was not available when this UV decontamination work was started, but this data will
970 impact future iterations of testing.

971 A ≥8 $\log_{10}$ challenge level was initially set for Φ6 testing because measurements with
972 high concentrations of microbes greatly increase the confidence in inactivation and mitigate the
973 risk of incomplete decontamination (Hamilton et al 2013). Furthermore, coronavirus nasal swabs
974 showed >8 $\log_{10}$ virus per swab as calculated using a PCR assay (Leung et al. 2020; Stadnytskyi
975 et al. 2020), and a recent human infection study showed 8.9 $\log_{10}$ genomic copies ml^{-1} from nasal
976 samples 5 d after infection (Killingley et al. 2022). The limitation of genomic sampling is that it
977 does not equate to infectious particles. However, an individual highly infected with SARS-CoV-

978 2 can emit >8 $\log_{10}$ virus particles in a 24 h period (Stadnytskyi et al. 2020). Extrapolation of
979 that data indicates that multiple personnel within confined spaces, limited ventilation, and low
980 humidity may generate considerably >8 $\log_{10}$ of infectious virus at any given point in time, and is
981 a critical considerations in both military and transportation applications. The infectious particle
982 data further justifies the need for ≥8 $\log_{10}$ challenge regardless of whether the virus is aerosolized
983 or on surfaces.

984 UV radiation does not fall under the United States Environmental Protection Agency
985 (EPA) jurisdiction for disinfection claims since it is not classified as a chemical disinfectant.
986 Nonetheless, for this study that began in 2020, the inactivation goal was reduced from ≥7 $\log_{10}$ to
987 ≥3 $\log_{10}$ inactivation during the COVID-19 pandemic to match the EPA N-list for
988 decontaminants. This was initially helpful because inactivation numbers for sanitation,
989 disinfection, and sterilization (Rutala et al. 1996) could be used for assessments of
990 decontaminants including UV. However, the 3 $\log_{10}$ kill threshold is now in question because a
991 very recent human infection study showed that only 10 $TCID_{50}$ of wild-type SARS-CoV-2
992 (equivalent to ~7 PFU) was needed to infect >50% of unvaccinated humans in a 36-volunteer
993 group with no prior infection (Killingley et al. 2022). This human infection study validates the
994 original quantitative objective to show enveloped virus inactivation of ≥7 $\log_{10}$ out of a ≥8 $\log_{10}$
995 challenge in order to increase decontamination confidence. These high kill
996 objectives/requirements are important to validate decontamination claims for respiratory
997 pathogens, which spread rapidly and continuously through air and likely also through surface
998 transfer. The wide variability in virus preparation and test methods and the associated results
999 published during COVID-19 has decreased end user confidence levels for evaluating
1000 decontaminants (Hadi et al. 2020). The limitation of direct SARS-CoV-2 virus testing is the lack
1001 of statistically significant test data with multiple independent preparations of virus at high virus
1002 titers (>10 $\log_{10}$ of virus ml^{-1} of culture medium at the time of virus harvest and without virus
1003 concentration or purification). These quantitative requirements need addressed in order to
1004 generate end user confidence that data can be reproduced (statistical accuracy) and that virus
1005 titers can match the virus stabilization and quantities that may be encountered in the
1006 environment.

1007 This background data indicates that detailed methods for mucus and aerosol testing of
1008 respiratory coronavirus virus will need to be defined, characterized, and developed for future
1009 iterations of decontamination testing. These should also include correlation testing among
1010 Biosafety Level 1, 2, and 3 enveloped viruses. Data from methods with increasingly higher
1011 confidence will improve the likelihood of end user acceptance of UV technologies. The work
1012 here showed that enveloped virus could be field tested at >8 $\log_{10}$ of stabilized enveloped virus
1013 using multiple preparations of virus and a live/dead assay. The quantitation could be reproduced
1014 and field tested with a 2-week data turnaround to provide an initial UV screening/selection. The
1015 UV test results here also showed that high UV dosages are needed to inactivate enveloped virus
1016 protected by environmental debris, and porous materials are difficult to decontaminate,
1017 particularly in comparison to purified virus alone. These limitations of UV are well documented
1018 by regulatory agencies, and those limitations also apply to SARS-CoV-2 (United States Food and
1019 Drug Administration 2021; United States Environmental Protection Agency 2021). Nonetheless,
1020 UV efficacy was measurable and very high dosages were effective even on relatively porous
1021 materials like cardboard. It is unlikely that UV would be useful for highly porous fabrics used to
1022 make bags, carpeting, and clothing, and those were not tested. In contrast, hot, humid air

1023 inactivates debris-laden microbes with similar kinetics regardless of material porosity (e.g. Buhr
1024 et al 2012, 2015, 2016, 2020). This is a hallmark difference between highly penetrative
1025 decontaminants and a surface decontaminant like UV.

1026 Anti-viral efficacy among the different UV devices ranged from no decontamination up
1027 to nearly achieving enveloped virus sterilization. Enormous variability in dosage and efficacy
1028 was measured within and among the different devices. The prototype medium conveyer
1029 generated the highest virus inactivation per dosage. Inoculated coupons were exposed to UV-C
1030 on three sides since the coupons were set on a flat surface during exposure in the conveyer. The
1031 big UV box also generated high levels of virus inactivation, but the medium conveyer was
1032 highest efficacy $dose^{-1}$. In contrast the handheld devices, pulsed Xenon devices, LEM, and the
1033 original prototypes A, B, and C, and modified prototype B were all evaluated with a UV source
1034 emitted from predominantly one direction with slightly varying angles of exposure. The
1035 increased angles of exposure in the conveyer and big box likely improved UV-C penetration.
1036 Hence, the unique geometry, design, and electronics of each device impacted the effectiveness
1037 above and beyond the wavelength and dosage.

1038 The variability seen among the various tested devices strongly indicates that all UV
1039 devices need to be measured for both UV dosage and for anti-viral efficacy before they are
1040 incorporated into decontamination protocols. The efficacy of a pulsed Xe bulb was measurable
1041 at close distances, but significantly lower than Hg bulbs. Pulsed Xe devices do have some
1042 practical advantages such as requiring minimal warm up time and no Hg toxicity. LEDs have the
1043 lowest hazard and lowest variability in UV output. However, the availability of UV LEDs has
1044 been limited, and UV dosages can also be limiting depending on the manufacturer, model, and
1045 the electronics and overall design of any given device. Longer wavelength UV (272 nm) showed
1046 the best efficacy in handheld devices, and 272 nm is more penetrating than short wavelengths.
1047 The 222 nm KrCl sources showed measurable efficacy in conjunction with proprietary prototype
1048 advancements. Additional testing with >8 $\log_{10}$ debris-laden virus is needed because the 222 nm
1049 KrCl testing was limited due to time and cost constraints.

1050 Finally, decontamination with UV comes with tradeoffs that affect the decision of the end
1051 user. The time of exposure needed to generate efficacy needs to be assessed by end users because
1052 long exposure times will limit the utility of UV, especially for handheld and air decontamination
1053 devices. Use of handheld UV devices is also very hard to standardize, which increases safety
1054 risks for end users (United States Food and Drug Administration 2021b). Another tradeoff to be
1055 assessed by end users is the need for cleaning and maintenance of UV devices to remove dirt and
1056 debris that accumulates on the radiation sources, and/or to change radiation sources. Devices and
1057 methods to monitor UV dosage over time are needed to assist in maintenance, a particularly
1058 important subject that is rarely addressed. Additional tradeoffs are ozone generation, which
1059 reached toxic levels up to 3.6 times higher than OSHA limits for some devices (Claus 2021), and
1060 operation times; Hg bulbs, in particular, require warmup times in order to reach a steady-state. In
1061 general, Hg bulbs generate a maximum intensity quickly, and then the intensities were stabilized
1062 at a lower level after a warm up period. The Hg devices would have performed better had only
1063 this initial dose been tested, but that data would not translate to practical application because it
1064 will be hard to standardize turn-on times for end users, especially for handhelds. Lastly, the end
1065 user needs an understanding of the organism(s) to be killed, how it is stabilized in the
1066 environment, and the impact of test methods on results, as these factors will impact confidence in

any application. Assessment of these tradeoffs will facilitate practical application of UV decontamination. UV has potential for augmenting current practices for limiting the spread of enveloped virus, but UV cannot and should not replace normal cleaning and hygienic practices or air filtration and ventilation. Equipment breakdowns/failures, electrical outages, and maintenance shortcomings are common, normal, and realistic. Hence, coronavirus test methods need to significantly improve in order to approximate realistic environmental conditions with debris-laden, dried, high titer virus and increase UV test confidence. As test standards, UV field validation methods, and UV sources improve, UV might become a more viable option for augmenting decontamination in some applications. Multiple layers of testing, including field validation testing such as that described herein, will be needed because of the extraordinary variability of UV output from different devices. In addition, methods to continuously monitor UV output and maintenance and cleaning guidelines are critical areas that need addressed.

ACKNOWLEDGEMENTS

This work was supported through funding and program support provided by Naval Sea Systems Command, Defense Innovation Unit, Naval Advanced Medical Devices, and the Defense Threat Reduction Agency (DTRA), Hazard Mitigation Capability Area (BA2 and 3 funds, Project Number CB10141). We thank Rich Wiersteiner, Jon Cofield, Heather Ichord, Janet Weir, Glenn Lawson, Chuck Bass, James Noah, John Aaron Miller, and Joe Schumer for support. We thank Jason A. Fallen, Dr. Joseph Hunt, Carlos Murillo, Kira Baugh, and Julie Caruana for outstanding technical support and/or assistance with editing the paper. This manuscript was approved for public release on 1/27/2022 as #6156; NSWCDD PN-22-00021 and 8/1/2022 as #6232; NSWCDD PN-22-00131 and will be released as a pre-print at bioRxiv (Buhr et al.).

COMPETING INTERESTS

None reported

REFERENCES

1095 ASTM International (formerly the Association for Standardized Test Materials). (2020).
1096 Guidance on SARS-CoV-2 Surrogate Selection. https://www.astm.org/COVID-19/ [Accessed
1097 on September 15, 2021].

1098 ASTM International (formerly the Association for Standardized Test Materials). (2018).
1099 Standard Practice for Evaluating Static and Cidal Chemical Decontaminants against *Bacillus*
1100 Spores using Centrifugal Filtration Tubes. ASTM Standard Practice E3178-18.

1101 ASTM International (formerly the Association for Standardized Test Materials). (2018).
1102 Standard Practice for Evaluating Efficacy of Vaporous Decontaminants Against *Bacillus* Spores
1103 Contained Within 0.2µm Filter-capped Tubes. ASTM Standard Practice E3092-18.

1104 ASTM International (formerly the Association for Standardized Test Materials). (2016).
1105 Evaluation of Effectiveness of Decontamination Procedures for Surfaces When Challenged with
1106 Droplets Containing Human Pathogenic Viruses. ASTM Standard Practice E2721-16.

1107 Aps, J.K.M. and Martens, L.C. (2005). Review: The physiology of saliva and transfer of drugs
1108 into saliva. Forensic Sci Int. 10;150(2-3):119-31. doi: 10.1016/j.forsciint.2004.10.026.

1109 Bibby, K., Casson, L.W., Stachler, E., and Haas, C.N. (2015). Ebola Virus Persistence in the
1110 Environment: State of the Knowledge and Research Needs. *Environ. Sci. Technol. Lett.* 2, 2−6.
1111 https://doi.org/10.1021/ez5003715

1112 Brakke, M. K. (1951). Density gradient centrifugation: A new separation technique. *J. Am.*
1113 *Chem. Soc.* 73:1847-1848.

1114 Brakke M.K.. (1967). Density-gradient centrifugation. Methods in Virology. Edited by: K
1115 Maramorosch and H Koprowski. New York, Academic Press, 2: 93-118.

1116 Bredberg, A., Gobom, J., Almstrand, A., Larsson, P., Blennow, K., Olin, A., and Mirgorodskaya,
1117 E. (2012). Exhaled endogenous particles contain lung proteins. *Clin. Chem. 58* (2), 431-440.

1118 Brown, J.S., Gordon, T., Price, O., and Asgharian, B. (2013) Thoracic and respirable particle
1119 definitions for human health risk assessment. *Particle and Fibre Toxicology* 10:1-12.
1120 http://www.particleandfibretoxicology.com/content/10/1/12

1121 Buhr, T. L., Young, A. A., Minter, Z.A., and Wells, C.M. (2012). Test method development to
1122 evaluate hot, humid air decontamination of materials contaminated with *Bacillus anthracis*
1123 ΔSterne and *B. thuringiensis* Al Hakam spores. *J Appl Microbiol* **113**, 1037–1051.
1124 https://doi.org/10.1111/j.1365-2672.2012.05423.x

1125 Buhr, T., Young, A.A., Johnson, C.A., Minter, Z., and Wells, C. (2014). Decontamination of
1126 materials contaminated with *Francisella philomiragia* or MS2 bacteriophage using PES-Solid, a
1127 solid source of peracetic acid. *J Appl Microbiol* **117,** 397-404. https://doi.org/10.1111/jam.12540

1128 Buhr, T., Young, A.A., Barnette, H., Minter, Z.A., Kennihan, N., McPherson, D.C., Johnson,
1129 C.A., Bohmke, M., DePaola, M., and Page, M. (2015). Test methods and response surface
1130 models for hot, humid air decontamination of materials contaminated with dirty spores of
1131 *Bacillus anthracis* ΔSterne and *B. thuringiensis* Al Hakam. *J. Appl. Microbiol.* 119, 1263-1277.

1132 Buhr, T., Young, A., Bensman, M., Minter, Z., Kennihan, N., Johnson, C., Bohmke, M.,
1133 Borgers-Klonkowski, E., Osborn, E., Avila, S., Theys, A., and Jackson, P. (2016). Hot, humid air
1134 decontamination of a C-130 aircraft contaminated with spores of two acrystalliferous *Bacillus*
1135 *thuringiensis* strains, surrogates for *Bacillus anthracis*. *J. Appl. Microbiol*. 120, 1074-1084.
1136 https://doi.org/10.1111/jam.13055

1137 Buhr T. L., Young A. A., Borgers-Klonkowski E., Kennihan N. L., Barnette H. K., Minter Z. A.,
1138 Bohmke M. D., Osborn E. B., Hamilton S. M., Kimani M. B., Hammon M. W., Miller C. T.,
1139 Mackie R. S., Innocenti J. M., Bensman M. D., Gutting B. W., Lilly S. D., Hammer E. E., Yates
1140 V. L., and Luck B. B. (2020). Hot, Humid Air Decontamination of Aircraft Confirmed That High
1141 Temperature and High Humidity Are Critical for Inactivation of Infectious, Enveloped
1142 Ribonucleic Acid (RNA) Virus. *Front Bioeng Biotechnol.* Oct 23;8:592621.
1143 https://doi.org/10.3389/fbioe.2020.592621

1144 Claus, H. (2021) Ozone Generation by Ultraviolet Lamps. *Photochem Photobiol* 97, 471-476.

1145 Chan, K. H., Malik Peiris, J. S., Lam, S. Y., Poon, L. L. M. , Yuen, K. Y., and Seto, W. H.
1146 (2011). The Effects of Temperature and Relative Humidity on the Viability of the SARS
1147 Coronavirus. *Adv Virology*, Article ID 734690, 7 pages. https://doi.org/10.1155/2011/734690

1148 Corfield, A.P. (2015) Mucins: A biologically relevant glycan barrier in mucosal protection.
1149 *Biochim Biophys Acta*. 1850 *(1)*, 236-52. doi: 10.1016/j.bbagen.2014.05.003.

1150 Cox, C.S., and Wathes, C.M. (Eds.). (1995). Bioaerosols Handbook (1st ed.). CRC Press.
1151 https://doi.org/10.1201/9781003070023

1152 de Carvalgo, N.A., Stachler, E.N., Cimabue, N., and Bibby, K. (2017). Evaluation of Phi6
1153 persistence and suitability as an enveloped virus surrogate. *Environ. Sci. Technol*. 51 (15), 8692–
1154 8700. https://doi.org/10.1021/acs.est.7b01296

1155 Fedorenko, A., Grinberg, M., Orevi, T., and Kashtan, N. (2020). Survival of the enveloped
1156 bacteriophage Phi6 (a surrogate for SARS-CoV-2) in evaporated saliva microdroplets deposited
1157 on glass surfaces. *Scientific Reports* 10:22419. https://doi.org/10.1038/s41598-020-79625-z

1158 Fenn, E. A. (2001). Pox Americana: The Great Smallpox Epidemic of 1775-82. New York: Hill
1159 and Wang.

1160 Gallandat, K. and Lantagne, D. (2017). Selection of a Biosafety Level 1 (BSL-1) surrogate to
1161 evaluate surface disinfection efficacy in Ebola outbreaks: Comparison of four bacteriophages.
1162 *PLOS ONE*. 12(5). https://doi.org/10.1371/journal.pone.0177943

1163 Goldsmith, C.S., Tatti, K.M., Ksiazek, T.G., Rollin, P.E., Comer, J.A., Lee, W.W., Rota, P.A.,
1164 Bankamp, B., Bellini, W.J., and Zaki, S.R. (2004). Ultrastructural characterization of SARS
1165 coronavirus. *Emerging Infectious Diseases*. 10 (2): 320-326. doi:10.3201/eid1002.030913

1166 Greiff D., Blumenthal H., Chiga, M., and Pinkerton, H. (1954). The effects on biologic materials
1167 of freezing and drying by vacuum sublimation II. Effect on influenza virus. *J Exptl Med* 100(1):
1168 89-101.

1169 Greiff D. and Rightel, W. (1966). Freezing and freeze-drying of viruses In: HT Meryman (Eds.).
1170 Cryobiology. Academic Press, Inc, New York, USA. pp. 697-728.

1171 Hadi, J., Dunowska, M., Wu, S., and Brightwell, G. (2020). Control Measures for SARS-CoV-2:
1172 A Review on Light-Based Inactivation of Single-Stranded RNA Viruses. *Pathogens* 9: 737-767;
1173 https://doi.org/10.3390/pathogens9090737

1174 Hamilton, M., Hamilton, G., Goeres, D., and Parker, A. (2013). Guidelines for the statistical
1175 analysis of a collaborative study of a laboratory disinfectant product performance test
1176 method. *JAOAC International* 96 (5), 1138-1151. https://doi.org/10.5740/jaoacint.12-217

1177 Heimbuch, B.K., Wallace, W.H., Kinney, K., Lumley, A.E., Wu, C.Y., Woo, M.H., and Wander,
1178 J.D. (2011). A pandemic influenza preparedness study: use of energetic methods to
1179 decontaminate filtering facepiece respirators contaminated with H1N1 aerosols and droplets. *Am*
1180 *J Infect Control* 39, e1-9.

1181 Heßling, M., Hönes, K., Vatter, P., and Lingenfelder, C. (2020). Ultraviolet irradiation doses for
1182 coronavirus inactivation – review and analysis of coronavirus photoinactivation studies. *GMS*
1183 *Hygiene and Infection Control* 2020, Vol. 15, ISSN 2196-5226
1184 https://dx.doi.org/10.3205%2Fdgkh000343

1185 Hendley, J.O., Wenzel, R.P., and Gwaltney, J.M., Jr. (1973). Transmission of Rhinovirus Colds
1186 by Self-Inoculation. *N Engl J Med* 288:1361–1364.

1187 Hofer, S., Hofstätter, N., Duschl, A., and Himly, M. (2021). SARS-CoV-2-Laden Respiratory
1188 Aerosol Deposition in the Lung Alveolar-Interstitial Region Is a Potential Risk Factor for Severe
1189 Disease: A Modeling Study. *J. Pers. Med*. 11, 431. https://doi.org/10.3390/jpm11050431

1190 Killingley, B., Mann, A., Kalinova, M., Boyers, A., Goonawardane, N., Zhou, J., Lindsell, K.,
1191 Hare, S.S., Brown, J., Frise, R., Smith, E., Hopkins, C., Noulin, N., Londt, B., Wilkinson, T.,
1192 Harden, S., McShane, H., Baillet, M., Gilbert, A., Jacobs, M., Charman, C., Mande, P., Nguyen-
1193 Van-Tam, J.S., Semple, M.G., Read, R.C., Ferguson, N.M., Openshaw, P.J., Rapeport, G.,
1194 Barclay, W.S., Catchpole, A.P., and Chiu, C. (2022). Safety, tolerability and viral kinetics during
1195 SARS-CoV-2 human challenge. Research Square pre-print, 1-27. DOI:
1196 https://doi.org/10.21203/rs.3.rs-1121993/v1

1197 Kratochvil, M.J., Kaber, G., Demirdjian, S., Cai, P.C., Burgener, E.B., Nagy, N., Barlow, G.L.,
1198 Popescu, M., Nicolls, M.R., Ozawa, M.G., Regula, D.P., Pacheco-Navarro, A.E., Yang, S., de

1199 Jesus Perez, V.A., Karmouty-Quintana, H., Peters, A.M., Zhao, B., Buja, M.L., Johnson, P.Y.,
1200 Vernon, R.B., Wight, T.N., Stanford COVID-19 Biobank Study Group, Milla, C.E., Rogers,
1201 A.J., Spakowitz, A.J., Heilshorn, S.C., and Bollyky. P.L. (2022) Biochemical, biophysical, and
1202 immunological characterization of respiratory secretions in severe SARS-CoV-2 infections. *JCI*
1203 *Insight* 7(12):e152629. https://doi.org/10.1172/jci.insight.152629

1204 Lai, S.K., Wang, Y., Wirtz, D., and Hanes, J. (2009) Micro- and macrorheology of mucus. *Adv*
1205 *Drug Deliv Rev.* 2009, 61 *(2)*, 86-100. doi:10.1016/j.addr.2008.09.012.

1206 Leung, N.H.L., Chu, D.K.W., Shiu, E.Y.C., Chan, K.-H., McDevitt, J.J., Hau, B.J.P., Yen, H.-L.,
1207 Li, Y., Ip, D.K.M., Peiris, J.S.M., Seto, W.H., Leung, G.M., Milton, D.K., and Cowling, B.J.
1208 (2020). Respiratory Virus Shedding in Exhaled Breath and Efficacy of Face Masks. *Nature*
1209 *Medicine* 26, 676-680. https://doi.org/10.1038/s41591-020-0843-2

1210 Malenovska, H. (2014). The influence of stabilizers and rates of freezing on preserving of
1211 structurally different animal viruses during lyophilization and subsequent storage. *J Appl*
1212 *Microbiol* 117, 1810—1819. https://doi.org/10.1111/jam.12654

1213 Masters, P.S. (2006). The molecular biology of coronaviruses. *Advances in Virus Research*. 66:
1214 193–292. doi:10.1016/S0065-3527(06)66005-3

1215 McDonnell, G. and Burke, P. (2011). Disinfection: is it time to reconsider Spaulding? *J. Hosp.*
1216 *Inf.* 78, 163–170. doi: 10.1016/j.jhin.2011.05.002 https://doi.org/10.1016/j.jhin.2011.05.002

1217 Memarzadeh, F. (2021). A Review of Recent Evidence for Utilizing Ultraviolet Irradiation
1218 Technology to Disinfect Both Indoor Air and Surfaces. *Applied Biosafety*. 26(1): 52-56.
1219 http://doi.org/10.1089/apb.20.0056

1220 Mindich, L. (2004). Packaging, replication and recombination of the segmented genomes of
1221 bacteriophage Φ6 and its relatives. *Virus Research*. 101, 83–92.
1222 https://doi.org/10.1016/j.viruses.2003.12.008

1223 Niazi, S., Groth, R. Spann, K., and Johnson, G.R. (2021). The role of respiratory droplet
1224 physiochemistry in limiting and promoting the airborne transmission of human coronaviruses: A
1225 critical review. *Environ. Pollut.* **2021**, *276* (115767).

1226 Raiszadeh, M. and Adeli, B. (2020). A Critical Review on Ultraviolet Disinfection Systems
1227 against COVID-19 Outbreak: Applicability, Validation, and Safety Considerations. *ACS*
1228 *Photonics.* 7 (11):2941-2951. https://doi.org/10.1021/acsphotonics.0c01245

1229 Riddell, S., Goldie, S., Hill, A., Eagles, D., and Drew, T.W. (2020) The effect of temperature on
1230 persistence of SARS-CoV-2 on common surfaces. *Virol J.* 7:17(1):145. doi: 10.1186/s12985-
1231 020-01418-7.

1232 Rutala, W.A. and APIC Committee (1996) APIC Guideline for selection and use of disinfectants.
1233 *Am J Infect Cont* 24:313-342. https://doi.org/10.1016/S0196-6553(96)90066-8

1234 Stadnytskyi, V., Bax, C. E., Bax, A., and Anfinrud, P. (2020). The airborne lifetime of small
1235 speech droplets and their potential importance in SARS-CoV-2 transmission. *Proc Natl Acad Sci*
1236 117(2), 11875-11877. https://doi.org/10.1073/pnas.2006874117

1237 Tseng, C.C. and Li, C.S. (2005). Inactivation of virus-containing aerosols by ultraviolet
1238 germicidal irradiation. *Aerosol Sci. Technol*. 39: 1136–1142.
1239 https://dx.doi.org/10.1080%2F15459620701329012

1240 Uchiho, Y., Goto, Y., Kamahori, M., Aota, T., Moriasaki, A., Hosen, Y., and Koda, K. (2015)
1241 Far-ultraviolet absorbance detection of sugars and peptides by high-performance liquid
1242 chromatography. *J. Chromatogr.* 1424:86-91. doi: 10.1016/j.chroma.2015.11.006.

1243 United States Environmental Protection Agency. (2021). Disinfecting Surfaces with UV Light to
1244 Reduce Exposure to SARS-CoV-2. https://www.epa.gov/covid19-research/disinfecting-surfaces-
1245 uv-light-reduce-exposure-sars-cov-2. [Accessed on September 15, 2021].

1246 United States Food and Drug Administration. (2021). UV Lights and Lamps: Ultraviolet-C
1247 Radiation, Disinfection, and Coronavirus. https://www.fda.gov/medical-devices/coronavirus-
1248 covid-19-and-medical-devices/uv-lights-and-lamps-ultraviolet-c-radiation-disinfection-and-
1249 coronavirus. [Accessed on September 15, 2021].

1250 United States Food and Drug Administration. (2021b). Risk of Exposure to Unsafe Levels of
1251 Radiation with Safe-T-Lite UV WAND: FDA Safety Communication.
1252 https://www.fda.gov/medical-devices/safety-communications/risk-exposure-unsafe-levels-
1253 radiation-safe-t-lite-uv-wand-fda-safety-communication. [Accessed on July 20, 2022].

1254 van Doremalen, N., Bushmaker, T., and Munster, V. J. (2013). Stability of Middle East
1255 respiratory syndrome coronavirus (MERS-CoV) under different environmental conditions. *Euro*
1256 *Surveill*. 18(38):pii=20590. https://doi.org/10.2807/1560-7917.ES2013.18.38.20590

1257 Van Etten, J., Lane, L., Gonzalez, C., Partridge, J., and Vidaver, A. (1976). Comparative
1258 properties of bacteriophage phi6 and phi6 nucleocapsid. *J. Virol*. 18(2), 652–658.

1259 Vejerano, E. P. and Marr, L. C. (2018). Physico-chemical characteristics of evaporating
1260 respiratory fluid droplets. *J. R. Soc. Interface* 15:20170939 http://doi.org/10.1098/rsif.2017.0939

1261 Vidaver, A.K., Roski, R.K., and Van Etten, J.L. (1973). Bacteriophage phi6: a lipid-containing
1262 virus of *Pseudomonas phaseolicola*. *J. Virol*. 11(5), 799-805.

1263 Weber, T. P. and Stilianakis, K. I. (2008). Inactivation of influenza A viruses in the environment
1264 and modes of transmission: A critical review. *J. Inf.* 57, 361-373. doi: 10.1016/j.jinf.2008.08.013
1265 https://doi.org/10.1016/j.jinf.2008.08.013

1266 Wiggington, K.R., Pecson, B.M., Sigstam, T., Bosshard, F., and Kohn, T. (2012). Virus
1267 inactivation mechanisms: impact of disinfectants on virus function and structural integrity.
1268 *Environ. Sci. Technol*. 46(21), 12069-12078. https://doi.org/10.1021/es3029473

1269 Williams, O.W., Sharafkhaneh, A., Kim, V., Dickey, B.F., and Evans, C.M. (2006). Airway
1270 Mucus From Production to Secretion. *Am. J. Respir. Cell. Mol. Biol*. 34, 527–536.
1271 https://doi.org/10.1165/rcmb.2005-0436sf

1272 Znamenskaya, Y., Sotres, J., Engblom, J., Arnebrant, T., and Kocherbitov, V. Effect of
1273 Hydration on the Structural and Thermodynamic Properties of Pig Gastric and Bovine
1274 Submaxillary Mucins. *J. Phys. Chem.* **2012**, 116 (16), 5047-5055. doi: 10.1021/jp212495t

Table 2. Dosage and efficacy of handheld, room, and chamber-type devices showing $\log_{10}$ reduction data based on the steady state emission, not peak emission. Legend: White (low decontamination) = Fail <2 $\log_{10}$; Yellow (sanitation) = Fail ≥2 $\log_{10}$, <3 $\log_{10}$; Light Blue (disinfection) = Pass ≥ 3 $\log_{10}$; and Dark Blue (approaching virus sterilization) = Pass ≥ 6 $\log_{10}$. N/A – dosage measurements had no meaning because of the broad-spectrum Xe source.

Name	Description	Dosage (mJ cm^{-2})	Exposure Distance	Exposure Time	Efficacy (Log_{10} Reduction after an >8 $\log_{10}$ challenge of live Φ6)				
					SS 304	NTC	Cardboard	*PMMA or ABS plastic	Polyurethane
GermAway UV 18W Handheld	2 12.7 cm Hg U-shape bulbs in handheld device 254 nm UV-C MSRP $100	101.2	5 cm	10 s	2.5 ± 0.1	2.0 ± 0.0	1.9 ± 0.0	1.9 ± 0.0	2.0 ± 0.0
		202.4	5 cm	20 s	4.3 ± 0.2	3.1 ± 0.2	2.0 ± 0.1	4.5 ± 0.1	3.3 ± 0.1
GermAway UV 35W Handheld	2 22.5 cm Hg twin tube bulbs in handheld device 254 nm UV-C MSRP $450	13.8	5 cm	2 s	0.3 ± 0.0	0.2 ± 0.0	0.3 ± 0.0	0.3 ± 0.0	0.3 ± 0.0
		34.5	5 cm	5 s	0.9 ± 0.1	0.6 ± 0.0	0.7 ± 0.0	0.8 ± 0.1	0.7 ± 0.0
		69.0	5 cm	10 s	1.4 ± 0.1	1.2 ± 0.1	1.2 ± 0.0	1.3 ± 0.0	1.1 ± 0.1
272 nm Prototype Handheld	8 LED strips divided by angled plastic in handheld device 272 nm UV-C	31.2	5 cm	2 s	3.0 ± 0.3	1.6 ± 0.2	1.6 ± 0.1	1.6 ± 0.2	1.6 ± 0.2
		78.0	5 cm	5 s	5.2 ± 0.1	2.8 ± 0.1	2.5 ± 0.2	3.1 ± 0.2	2.0 ± 0.9
		156	5 cm	10 s	6.2 ± 0.4	3.8 ± 0.2	2.4 ± 0.1	4.9 ± 0.2	4.7 ± 0.5
222 nm Excimer Prototype Handheld	3 lamp modules attached to 2.54 cm thick plastic panel, in handheld device 222 nm UV-C	5.9	5 cm	2 s	0.6 ± 0.1	0.4 ± 0.2	0.1 ± 0.1	0.3 ± 0.1	0.3 ± 0.1
		14.8	5 cm	5 s	0.9 ± 0.2	0.1 ± 0.1	0.5 ± 0.1	0.5 ± 0.1	0.6 ± 0.2
		29.6	5 cm	10 s	1.1 ± 0.2	0.9 ± 0.1	0.6 ± 0.1	0.9 ± 0.1	1.1 ± 0.1
Mounted Pulsed-Xenon Prototype	Pulsed-Xe bulb in small housing ceiling, wall, or tripod-mounted Broad-spectrum UV-B, UV-C	N/A	0.5 m	15 min	1.4 ± 0.1	1.1 ± 0.1	1.1 ± 0.1	1.5 ± 0.1	N/A
			0.5 m	30 min	2.3 ± 0.1	2.3 ± 0.1	1.6 ± 0.1	2.9 ± 0.1	N/A
			0.5 m	60 min	5.2 ± 0.2	3.2 ± 0.3	2.4 ± 0.2	5.2 ± 0.2	N/A
			1 m	15 min	0.5 ± 0.0	0.4 ± 0.1	0.4 ± 0.1	0.3 ± 0.1	N/A
			1 m	30 min	0.8 ± 0.0	0.7 ± 0.0	0.7 ± 0.1	0.7 ± 0.0	N/A
			1 m	60 min	1.5 ± 0.1	1.3 ± 0.1	1.0 ± 0.0	1.3 ± 0.1	N/A
			2 m	15 min	0.0 ± 0.1	0.1 ± 0.1	0.2 ± 0.0	0.1 ± 0.0	N/A
			2 m	30 min	0.1 ± 0.0	0.0 ± 0.0	0.2 ± 0.0	0.2 ± 0.1	N/A
			2 m	60 min	0.3 ± 0.0	0.2 ± 0.1	0.3 ± 0.0	0.2 ± 0.0	N/A
Xenex Lightstrike	1 pulsed-Xe bulb mounted on rolling cart Broad-spectrum UV-B, UV-C MSRP $125,000	N/A	178 cm	5 min	0.8 ± 0.1	0.4 ± 0.0	0.5 ± 0.0	0.5 ± 0.0	N/A
		N/A	178 cm	20 min	1.7 ± 0.0	1.5 ± 0.1	1.3 ± 0.0	2.2 ± 0.1	NA
Light Emitting Module (LEM)	20 Hg bulbs mounted in a ring on rolling cart 254 nm UV-C MSRP $95,000	60	263 cm	4 min 22 s	3.1 ± 0.3	2.6 ± 0.2	1.6 ± 0.1	2.5 ± 0.2	2.1 ± 0.1
		100	263 cm	7 min 2 s	4.6 ± 0.5	2.7 ± 0.2	2.2 ± 0.1	2.7 ± 0.2	3.1 ± 0.1
		140	263 cm	9 min 33 s	5.3 ± 0.5	3.4 ± 0.1	2.7 ± 0.1	4.0 ± 0.2	3.9 ± 0.1
Medium Conveyer Prototype	Chamber lined on 4sides with Hg bulbs, powered conveyer belt to move items through 254 nm UV-C	60	62 cm	20 s	6.1 ± 0.2	4.5 ± 0.1	2.9 ± 0.3	4.8 ± 0.2	5.3 ± 0.1
		100	62 cm	32 s	7.6 ± 0.3	4.4 ± 0.2	2.9 ± 0.2	6.3 ± 0.2	7.1 ± 0.3
		140	62 cm	44 s	7.1 ± 0.4	4.3 ± 0.5	2.6 ± 0.1	6.3 ± 0.3	6.3 ± 0.3
		13.7	62 cm	8 s	1.6 ± 0.2	1.4 ± 0.1	1.3 ± 0.1	1.4 ± 0.1	N/A
		23.8	62 cm	16 s	2.7 ± 0.2	1.9 ± 0.1	1.8 ± 0.1	2.1 ± 0.1	N/A
		40.0	62 cm	24 s	3.5 ± 0.3	2.8 ± 0.1	2.5 ± 0.1	2.9 ± 0.1	N/A
		56.2	62 cm	32 s	4.7 ± 0.4	3.2 ± 0.2	2.9 ± 0.1	3.7 ± 0.1	N/A
Big Box Prototype	Chamber lined on sides and top with Hg bulbs (total 320) 254 nm UV-C	377-729	17 cm	2 min	5.4 ± 0.2	3.6 ± 0.3	3.1 ± 0.2	5.7 ± 0.1	5.4 ± 0.3

*ABS plastic was tested for the mounted pulsed Xe and the Big Box prototypes. PMMA plastic was tested for the other devices.

Table 3. Dosage and efficacy of handheld, room, and chamber-type devices showing $\log_{10}$ survival data based on the steady state emission, not peak emission**.** Legend: White (low decontamination) = Fail <2 $\log_{10}$; Yellow (sanitation) = Fail ≥2 $\log_{10}$, <3 $\log_{10}$; Light Blue (disinfection) = Pass ≥ 3 $\log_{10}$; and Dark Blue (approaching virus sterilization) = Pass ≥ 6 $\log_{10}$. N/A – dosage measurements had no meaning because of the broad-spectrum Xe source.

Name	Description	Dosage (mJ cm^{-2})	Exposure Distance	Exposure Time	Log_{10} Survival after a >8 $\log_{10}$ challenge of live Φ6					
					Inoculum	SS 304	NTC	Cardboard	*PMMA or ABS plastic	Polyurethane
GermAway UV 18W Handheld	2 12.7 cm U-shape Hg bulbs in handheld device 254 nm UV-C MSRP $100	101.2	5 cm	10 s	8.4 +/- 0.1	5.9 ± 0.5	6.4 ± 0.1	6.5 ± 0.1	5.5 ± 1.1	6.4 ± 0.1
		202.4	5 cm	20 s	8.2 +/- 0.0	3.9 ± 0.4	5.0 ± 0.4	6.1 ± 0.3	3.7 ± 0.3	5.1 ± 0.2
GermAway UV 35W Handheld	2 22.5 cm twin tube Hg bulbs in handheld device 254 nm UV-C MSRP $450	13.8	5 cm	2 s	8.2 +/- 0.1	7.8 ± 0.2	7.9 ± 0.1	7.8 ± 0.1	7.8 ± 0.2	7.8 ± 0.1
		34.5	5 cm	5 s		7.2 ± 0.2	7.5 ± 0.1	7.3 ± 0.1	7.3 ± 0.3	7.4 ± 0.1
		69.0	5 cm	10 s		6.6 ± 0.3	6.9 ± 0.2	6.9 ± 0.1	6.8 ± 0.2	7.0 ± 0.2
272 nm Prototype Handheld	8 LED strips divided by angled plastic in handheld device 272 nm UV-C	31.2	5 cm	2 s	8.5 +/- 0.2	5.5 ± 0.6	7.0 ± 0.3	6.9 ± 0.2	6.9 ± 0.3	6.9 ± 0.4
		78.0	5 cm	5 s		3.3 ± 0.0	5.7 ± 0.1	6.0 ± 0.4	5.4 ± 0.3	6.5 ± 1.9
		156	5 cm	10 s		2.3 ± 0.7	4.7 ± 0.3	6.1 ± 0.1	3.6 ± 0.5	3.8 ± 0.9
222 nm Excimer Prototype Handheld	3 lamp modules attached to 2.54 cm thick plastic panel, in handheld device 222 nm UV-C	5.9	5 cm	2 s	8.3 +/- 0.2	7.7 ± 0.2	7.9 ± 0.3	8.2 ± 0.1	8.0 ± 0.1	7.9 ± 0.0
		14.8	5 cm	5 s		7.4 ± 0.3	8.2 ± 0.1	7.8 ± 0.1	7.8 ± 0.2	7.6 ± 0.3
		29.6	5 cm	10 s		7.1 ± 0.4	7.1 ± 0.4	7.6 ± 0.1	7.4 ± 0.2	7.1 ± 0.1
Mounted Pulsed-Xenon Prototype	Pulsed-Xe bulb in small housing ceiling, wall, or tripod-mounted Broad-spectrum UV-B, UV-C	N/A	0.5 m	15 min	8.2 +/- 0.1	6.8 ± 0.2	7.0 ± 0.2	7.1 ± 0.2	6.7 ± 0.1	N/A
			0.5 m	30 min		5.9 ± 0.3	5.8 ± 0.3	6.6 ± 0.1	5.3 ± 0.2	N/A
			0.5 m	60 min		2.9 ± 0.4	5.0 ± 0.8	5.7 ± 0.5	3.0 ± 0.6	N/A
			1 m	15 min		7.7 ± 0.1	7.7 ± 0.2	7.7 ± 0.1	7.8 ± 0.1	N/A
			1 m	30 min		7.4 ± 0.1	7.5 ± 0.0	7.4 ± 0.1	7.4 ± 0.1	N/A
			1 m	60 min		6.7 ± 0.2	6.8 ± 0.2	7.2 ± 0.1	6.8 ± 0.2	N/A
			2 m	15 min		8.2 ± 0.1	8.1 ± 0.1	8.0 ± 0.1	8.1 ± 0.0	N/A
			2 m	30 min		8.1 ± 0.1	8.1 ± 0.1	8.0 ± 0.1	8.0 ± 0.1	N/A
			2 m	60 min		7.9 ± 0.0	7.9 ± 0.1	7.8 ± 0.1	7.9 ± 0.1	N/A
Xenex Lightstrike	1 pulsed-Xe bulb mounted on rolling cart Broad-spectrum UV-B, UV-C MSRP $125,000	N/A	178 cm	5 min	8.4 +/- 0.0	7.6 ± 0.2	8.0 ± 0.1	7.9 ± 0.1	7.8 ± 0.1	N/A
		N/A	178 cm	20 min		6.7 ± 0	6.9 ± 0.3	7.1 ± 0.0	6.2 ± 0.1	N/A
Light Emitting Module (LEM)	20 Hg bulbs mounted in a ring on rolling cart 254 nm UV-C MSRP $95,000	60	263 cm	4 min 22 s	8.4 +/- 0.2	5.3 ± 0.6	5.8 ± 0.5	6.8 ± 0.2	5.9 ± 0.5	6.3 ± 0.1
		100	263 cm	7 min 2 s		3.8 ± 1.1	5.7 ± 0.5	6.2 ± 0.2	5.7 ± 0.4	5.3 ± 0.1
		140	263 cm	9 min 33 s		3.1 ± 1.1	5.0 ± 0.3	5.8 ± 0.2	4.4 ± 0.3	4.6 ± 0.2
Medium Conveyer Prototype	Chamber lined on 4 sides with Hg bulbs, powered conveyer belt to move items through 254 nm UV-C	60	62 cm	20 s	8.2 +/- 0.1	2.1 ± 0.4	3.7 ± 0	5.3 ± 0.6	3.4 ± 0.4	2.9 ± 0.1
		100	62 cm	32 s		0.6 ± 0.6	3.8 ± 0.5	5.3 ± 0.4	2.0 ± 0.4	1.1 ± 0.7
		140	62 cm	44 s		1.1 ± 0.8	3.9 ± 1.1	5.6 ± 0.1	1.9 ± 0.6	0.9 ± 0.5
		13.7	62 cm	8 s	8.4 +/- 0.2	6.8 ± 0.4	7.0 ± 0.1	7.1 ± 0.1	7.0 ± 0.1	N/A
		23.8	62 cm	16 s		5.6 ± 0.4	6.5 ± 0.1	6.5 ± 0.2	6.3 ± 0.1	N/A
		40.0	62 cm	24 s		4.8 ± 0.6	5.5 ± 0.2	5.8 ± 0.3	5.4 ± 0.2	N/A
		56.2	62 cm	32 s		3.7 ± 1.0	5.1 ± 0.4	5.5 ± 0.2	4.7 ± 0.1	N/A
Big Box Prototype	Chamber lined on sides and top with Hg bulbs (total 320) 254 nm UV-C	377-729	17 cm	2 min	8.4 +/- 0.1	3.0 ± 0.4	4.8 ± 0.6	5.3 ± 0.5	2.5 ± 0.3	3.0 ± 0.6
					8.2 +/- 0.1 (ABS plastic only)					

*ABS plastic was tested for the mounted pulsed Xe and the Big Box prototypes. PMMA plastic was tested for the other devices.

Table 4. Dosage and efficacy of room-air-irradiating prototypes showing $\log_{10}$ reduction data based on the average power from the bulb area, not the peaks. Legend: White (low decontamination) = Fail <2 $\log_{10}$; Yellow (sanitation) = Fail ≥2 $\log_{10}$, <3 $\log_{10}$; Light Blue (disinfection) = Pass ≥ 3 $\log_{10}$; and Dark Blue (approaching virus sterilization) = Pass ≥ 6 $\log_{10}$. N/A – dosage measurements had no meaning because of the broad-spectrum Xe source.

Name	Description	Dosage (mJ cm^{-2})	Exposure Distance (cm)	Exposure Time (s)	Efficacy (Log_{10} Reduction after a >8 $\log_{10}$ challenge of live Φ6)	
					SS 304	Quartz Glass
Ceiling-mounted prototype A: Original	2 Hg bulbs within enclosed chamber; fans circulate air through unit 254 nm UV-C	18.6	5	5	0.9 ± 0.1	NA
		37.2		10	1.3 ± 0.1	NA
		55.8		15	1.7 ± 0.1	NA
		12.9	10	5	0.6 ± 0.1	NA
		25.7		10	1.0 ± 0.1	NA
		38.6		15	1.3 ± 0.1	NA
		10.6	15	5	0.5 ± 0.1	NA
		21.1		10	0.8 ± 0.1	NA
		31.7		15	1.1 ± 0.1	NA
Wall-mounted device A: Modified	KrCl/Excimer lamp within enclosed chamber; fans circulate air through unit 222 nm UV-C	15.2	4	5	NA	5.5 ± 0.6
		30.5		10	NA	6.4 ± 0.3
		45.8		15	NA	6.6 ± 0.7
		6.9	10	5	NA	2.2 ± 0.2
		13.7		10	NA	4.6 ± 0.7
		20.6		15	NA	6.7 ± 0.2
		3.4	20	5	NA	1.3 ± 0.1
		6.8		10	NA	2.4 ± 0.3
		10.2		15	NA	4.0 ± 0.6
Wall-mounted prototype B: Original	Hg bulb within open sconce; fans circulate air through unit 254 nm UV-C	29.9	5	5	1.6 ± 0.1	NA
		59.8		10	2.5 ± 0.1	NA
		89.7		15	3.4 ± 0.1	NA
		15.8	10	5	1.1 ± 0.1	NA
		31.6		10	1.7 ± 0.1	NA
		47.4		15	2.3 ± 0.1	NA
		9.9	15	5	0.8 ± 0.1	NA
		19.7		10	1.3 ± 0.2	NA
		29.6		15	1.5 ± 0.1	NA
Wall-mounted prototype B:: Modified	KrCl/Excimer lamp within open sconce; fans circulate air through unit 222 nm UV-C	15.6	5	5	0.5 ± 0.1	NA
		31.2		10	0.9 ± 0.2	NA
		46.8		15	1.2 ± 0.3	NA
		7.5	15	5	0.6 ± 0.2	NA
		15.0		10	0.5 ± 0.3	NA
		22.5		15	0.9 ± 0.1	NA
		2.8	30.5	5	0.1 ± 0.1	NA
		5.6		10	0.2 ± 0.1	NA
		8.4		15	0.2 ± 0.2	NA
		0.2	61	5	0.0 ± 0.2	NA
		0.3		10	0.0 ± 0.2	NA
		0.5		15	0.1 ± 0.1	NA
		0.1	71	5	0.0 ± 0.1	NA
		0.2		10	0.0 ± 0.1	NA
		0.3		15	0.0 ± 0.1	NA
Wall-mounted prototype C	Hg bulb within open sconce; fans circulate air through unit 254 nm UV-C	16.6	5	5	0.9 ± 0.2	NA
		33.2		10	1.6 ± 0.0	NA
		49.8		15	2.2 ± 0.2	NA
		9.1	10	5	0.7 ± 0.1	NA
		18.2		10	0.9 ± 0.1	NA
		27.3		15	1.3 ± 0.1	NA
		6.4	15	5	0.5 ± 0.1	NA
		12.8		10	0.8 ± 0.0	NA
		19.2		15	1.2 ± 0.1	NA

Table 5. Dosage and efficacy of room-air-irradiating prototypes showing $\log_{10}$ survival data based on the average power from the bulb area, not the peaks. Legend: White (low decontamination) = Fail <2 $\log_{10}$; Yellow (sanitation) = Fail ≥2 $\log_{10}$, <3 $\log_{10}$; Light Blue (disinfection) = Pass ≥ 3 $\log_{10}$; and Dark Blue (approaching virus sterilization) = Pass ≥ 6 $\log_{10}$. N/A – dosage measurements had no meaning because of the broad-spectrum Xe source.

Name	Description	Dosage (mJ cm^{-2})	Exposure Distance (cm)	Exposure Time (s)	Log_{10} Survival after a >8 $\log_{10}$ challenge of live Φ6		
					Inoculum	SS 304	Quartz Glass
Ceiling-mounted Prototype A: Original	2 Hg bulbs within enclosed chamber; fans circulate air through unit 254 nm UV-C	18.6	5	5	8.2 +/- 0.0	7.3 ± 0.3	NA
		37.2		10		6.9 ± 0.1	NA
		55.8		15		6.5 ± 0.2	NA
		12.9	10	5		7.6 ± 0.2	NA
		25.7		10		7.2 ± 0.3	NA
		38.6		15		7.0 ± 0.1	NA
		10.6	15	5		7.8 ± 0.1	NA
		21.1		10		7.4 ± 0.3	NA
		31.7		15		7.1 ± 0.2	NA
Wall-mounted Prototype A: Modified	KrCl/Excimer lamp within enclosed chamber; fans circulate air through unit 222 nm UV-C	15.2	4	5	8.2 +/- 0.1	NA	2.7 ± 1.4
		30.5		10		NA	1.8 ± 0.7
		45.8		15		NA	1.6 ± 1.6
		6.9	10	5		NA	6.0 ± 0.5
		13.7		10		NA	3.5 ± 1.5
		20.6		15		NA	1.4 ± 0.4
		3.4	20	5		NA	6.8 ± 0.3
		6.8		10		NA	5.7 ± 0.7
		10.2		15		NA	4.1 ± 1.3
Wall-mounted Prototype B: Original	Hg bulb within open sconce; fans circulate air through unit 254 nm UV-C	29.9	5	5	8.2 +/- 0.0	6.7 ± 0.1	NA
		59.8		10		5.7 ± 0.2	NA
		89.7		15		4.8 ± 0.3	NA
		15.8	10	5		7.1 ± 0.2	NA
		31.6		10		6.5 ± 0.2	NA
		47.4		15		5.9 ± 0.3	NA
		9.9	15	5		7.5 ± 0.2	NA
		19.7		10		6.9 ± 0.4	NA
		29.6		15		6.7 ± 0.2	NA
Wall-mounted Prototype B:: Modified	KrCl/Excimer lamp within open sconce; fans circulate air through unit 222 nm UV-C	15.6	5	5	8.1 +/- 0.3	7.6 ± 0.1	NA
		31.2		10		7.2 ± 0.4	NA
		46.8		15		6.9 ± 0.6	NA
		7.5	15	5		7.6 ± 0.2	NA
		15.0		10		7.6 ± 0.6	NA
		22.5		15		7.2 ± 0.1	NA
		2.8	30.5	5		8.1 ± 0.1	NA
		5.6		10		7.9 ± 0.2	NA
		8.4		15		7.9 ± 0.2	NA
		0.2	61	5		8.1 ± 0.2	NA
		0.3		10		8.1 ± 0.2	NA
		0.5		15		8.0 ± 0.1	NA
		0.1	71	5		8.1 ± 0.1	NA
		0.2		10		8.1 ± 0.1	NA
		0.3		15		8.1 ± 0.2	NA
Wall-mounted Prototype C	Hg bulb within open sconce; fans circulate air through unit 254 nm UV-C	16.6	5	5	8.2 +/- 0.0	7.4 ± 0.3	NA
		33.2		10		6.7 ± 0.1	NA
		49.8		15		6.1 ± 0.3	NA
		9.1	10	5		7.5 ± 0.2	NA
		18.2		10		7.3 ± 0.2	NA
		27.3		15		6.9 ± 0.2	NA
		6.4	15	5		7.7 ± 0.1	NA
		12.8		10		7.4 ± 0.1	NA
		19.2		15		7.1 ± 0.1	NA